King Saud University

Arabian Journal of Chemistry

www.ksu.edu.sa
www.sciencedirect.com

ORIGINAL ARTICLE

A novel modification of ionic liquid mixture density based on semi-empirical equations using laplacian whale optimization algorithm

Hamidreza Bagheri [a,*], **Mohammad Sadegh Hosseini** [b,*], **Hossein Ghayoumi Zadeh** [c], **Behrouz Notej** [d], **Ali Fayazi** [c]

[a] *Department of Chemical Engineering, Faculty of Engineering, Shahid Bahonar University of Kerman, Kerman, Iran*
[b] *Department of Chemical Engineering, Faculty of Engineering, Vali-E-Asr University of Rafsanjan, Rafsanjan, Iran*
[c] *Department of Electrical Engineering, Faculty of Engineering, Vali-E-Asr University of Rafsanjan, Rafsanjan, Iran*
[d] *Department of Chemical Engineering, School of Chemical and Petroleum Engineering, Shiraz University, Shiraz, Iran*

Abstract The main motivation of this study is development of density prediction of mixture including ionic liquid (IL) using semi-empirical and cubic equations of state (CEoS). The considered systems are contained of 51 ILs, 41 solvents and 4626 data point in the wide temperature range (278.15–348.15 K), ionic liquid mole fraction (0.0040–0.9977) and atmospheric pressure. Six simple semi-empirical equations with different mixing rules and two CEoSs (Soave-Redlich-Kwong EoS and Patel-Teja EoS) is investigated to predict the IL-mixture density. For each semi-empirical equation, the coefficients are optimized using laplacian whale optimization algorithm based on cation-family. These generalized modifications have not been used to ILs beforehand consequently, the accuracy and appropriateness of these equations to predict IL-mixture density are unknown until now. The obtained results based on semi-empirical equations indicate that the performed modification provides low deviation of experimental data and can be applied by confidence in engineering and thermodynamic calculations. However, the results based on two CEoS show inacceptable accuracy.

© 2021 The Authors. Published by Elsevier B.V. on behalf of King Saud University. This is an open access article under the CC BY-NC-ND license (http://creativecommons.org/licenses/by-nc-nd/4.0/).

1. Introduction

In current years, the attention in green technology has led to the extension of a novel class of highly tunable and unique components that are called ionic liquids (IL). The ILs are the components that have revolutionized the corresponding researches and chemical industries. They are investigated as green chemical components that play a very significant role

ELSEVIER **Production and hosting by Elsevier**

Nomenclature

a	Attractive term parameter of equation of state [cm^6/mol^2]
a_i	Fitting parameters (i = 0, 1, 2, 3, 4)
AAPD	Average absolute percent deviation [-]
b	Repulsive term(co-volume) parameter of equation of state [cm^3/mol]
b_i	Fitting parameters (i = 0, 1, 2, 3, 4)
B	Dimensionless repulsive term parameter of equation of state [-]
c	Volume-translated parameter [cm^3/mol]
c_i	Fitting parameters (i = 0, 1, 2, 3)
C	Dimensionless volume-translated parameter of equation of state [-]
k_{ij}	Binary interaction parameter [-]
M_w	Solid molecular weight [g/mol]
N	Number of experimental data point
P	Pressure [bar]
R	Ideal gas constant [$bar.cm^3/K.mol$]
T	Temperature [K]
$T_r = T/T_c$	Reduced temperature [-]
V, v	Molar volume [cm^3/mol]
x	Mole fraction [-]
Z	Compressibility factor [-]

Greek letter

α	Temperature dependency coefficient of attractive term
η	Calculated critical compressibility factor [-]
ρ	Density [g/cm^3]
Ω	Patel-Teja Equation of state parameter coefficient
ω	Acentric factor [-]

Subscript

c	Critical
EoS	Equation of state
Exp.	Experimental
m	Mixture

Superscript

Calc.	Calculated
E	Excess
EoS	Equation of state
i	Component i
j	Component j

as a solvent to decrease applying of harmful, toxic and hazardous chemical components for the environment (Nishan et al., 2021). The main reason of increased considers on ILs is the aim of researchers to look for an appropriate alternative for volatile conventional organic solvents among the industries. Indeed, volatile conventional organic solvents are main environmental pollution resource in chemical industries (El shafiee et al., 2021). Although, all ILs are not completely considered as green solvents, some of ILs are even considerably toxic. Ionic liquids have involved a significant interest throughout the last three decades in the industrial and academic fields due to their unique properties (Agafonov et al., 2020; Omar et al., 2021). ILs are usually composed of inorganic or organic anions and an organic cation (Lian et al., 2016). According to cations, ILs are categorized to several categories like sulfonium, amino acids, phosphonium, guanidinium, ammonium, pyridazinium, piperazinium, oxazolidinium, tetrazolium, morpholinium, uranium, thiazolium, isoquinolinium, pyrroline, piperidinium, pyrrolidinium, pyridinium and imidazolium. Moreover, nitrate, perchlorate, bromide and chloride are simple anions and bis((trifluoromethyl)sulfonyl) imide, trifluoromethanesulfonate and lactate are complex anions (Bagheri et al., 2021; Evangelista et al., 2014; Xu et al., 2009). The ionic liquids properties will depend on the special combination of the anion and cation. The significant physicochemical features of ionic liquids like high electrochemical, thermal and chemical stability, non-flammability, low melting point and low vapor pressure (non-volatility) at moderate temperatures and pressures, high solvating power for non-polar and polar compounds have made ILs the exploration subject in many applications (Mohammadzadeh et al., 2020).

Designing equipment and chemical processes that involve ILs, needs accurate data on ILs thermo-physical features. The knowledge of ILs chemical and physical features is fundamental for ILs applications. Consequently, a number of scientists have investigated the thermodynamic properties of pure ILs and binary IL-mixture systems (Mesquita et al., 2019; Bagheri and Mohebbi, 2017). Until now, most investigations related to features of IL are limited to pure ones like viscosity, heat capacity, conductivity, surface tension and density. But, the usage of IL-mixture in engineering applications needs accurate detail about thermodynamic and physical features of ILs. The volumetric features refer to be related by substance volume change, such as expansibility, compressibility, excess molar volume, partial molar volume and density. ILs density is one of the most basic ILs volumetric features that is necessary in process design and calculations of metering of IL and it is interpreting interactions of intermolecular between solvent and ILs molecular (Tao et al., 2020). It is possible to calculate the ILs density accurately using experimental methods. However, as the experimental calculations are usually difficult, time consuming and costly consequently, the experimental calculations are not continuously possible (Tao et al., 2020; Bagheri et al., 2019; Paiva et al., 2019). Indeed, to develop process based on IL from the laboratory scale to industrial applications, the sufficient theoretical models to calculate ILs thermo-physical features must be considered (Bagheri and Ghader, 2017). In point of fact, the equipment design like liquid–liquid and vapor–liquid separation, energy and material balances including liquids, tower height calculations, rebuilders and condensers and storage vessels sizing, all need accurate liquid density values. Furthermore, other ILs features like surface tension or heat capacity, are sometimes correlated by density, so the reliable values of density permit one to calculate the mentioned features by an acceptable accuracy (Lian et al., 2016).

It is difficult to calculate features of all substances especially at various temperature and pressure or expensive and toxic components that maybe cause serious injuries for environment and human health. Thus, it is required to find out a method to calculate substances features. To solve the mentioned problem several estimation method was presented to estimate pure and IL-mixture. The presented methods are different from one case to another one and such correlations are based on some adjustable parameters, some of them are based on group contribution methods, equations of state and or machine learning methods (Abumandour et al., 2020; Yang et al., 2020; Bagheri et al., 2021).

Several semi-empirical equations were presented to calculate IL pure density such as Redlich-Kister polynomial equation, Lorentz-Lorenz equation, Tait equation and Wright equation and they have some fitting parameters (Lampreia et al., 2003; Valderrama and Zarricuetac, 2009; Geppert-Rybczyńska et al., 2010; I. Bahadur I, N. Deenadayalu, , 2011; Matkowska and Hofman, 2013; Bahadur et al., 2013; Govinda et al., 2013; Govinda et al., 2013; Singh et al., 2014; Huang et al., 2015). However, Hosseini et al. (Hosseini et al., 2013) presented the modified version of Spencer and Danner equation to predict IL-mixture density. The used data set was including 854 experimental data points and 14 binary mixtures. The obtained results indicated the performed modification had acceptable performance to predict IL-mixture density. Equations of state (EoS) and group contribution (GC) EoS are other sets of equations which were used to estimate the IL binary mixture (Abareshi et al., 2009; Wang et al., 2010; Li et al., 2011; Shen et al., 2011; Shahriari et al., 2012; Oliveira et al., 2012; Hosseini et al., 2012; Yousefi, 2012; Sheikhi-Kouhsar et al., 2015). EoSs are important tool to design in chemical engineering and supposed a developing role in the consideration of the fluid mixtures phase equilibria. However, the accuracy of some CEoSs is low to predict features of thermodynamic in a wide range of pressures and temperatures (Liu et al., 2020; Kamath et al., 2010; Ghoderao et al., 2019; Coquelet et al., 2016). The binary mixtures containing IL are complex systems, due to depend not only on molecular-molecular interaction, but also on the ion-molecular and ion-ion interactions. Cubic EoSs (CEoSs) consider only the attraction and repulsive interaction and they are unable to consider the other intermolecular forces (Panayiotou et al., 2019; Farrokh-Niae et al., 2008; Kukreja et al., 2021; Secuianu et al., 2008; Lopez-Echeverry et al., 2017). Therefore, the obtained results of IL-mixture density based on CEoSs have systematic deviation. Although some corrections like volume-translated to decrease systematic deviation was performed (Sheikhi-Kouhsar et al., 2015). The statistical associating fluid theory (SAFT) family EoS is according to perturbation theory. The SAFT family EoSs consider almost all intermolecular forces and presented the real form of intermolecular forces of components. However, computer programing of SAFT family EoSs are time consuming and need advance numerical methods (Perdomo et al., 2021; J. Gross J, G. Sadowski, , 2002; Bülow et al., 2021). Also, GC method required an accurate and perfect knowledge of the IL structure and it is time consuming and complex. Furthermore, the model fails and is considerably limited when applying large substructures as group parameters (Qiao et al., 2010; Peng et al., 2017; Chen et al., 2019). Machine learning method is another advantageous tool to predict properties pure and mixture IL and it is extensively accepted as estimation technique (Venkatraman and Alsberg, 2017). The relationship between the properties is nonlinear and the machine learning method is a significantly able algorithm to estimate certain properties like density by learning the relation between the input data (for instance temperature, pressure and critical features) and output data (like density) (Zhang et al., 2006; Yusuf et al., 2021). Also, the accuracy of the obtained results depends on the size of the training data set and the most important weakness of the machine learning method is low capability to predict the future performance of the network (generalization) (Low et al., 2020).

Density is one of the basic features of ionic liquid mixtures that would be useful in understanding intermolecular interactions between molecules of ionic liquid and solvent. The main purpose of this study is to develop a more accurate and reliable methods for estimating density of IL + solvent binary system. Consequently, the density of 130 various IL + solvent binary mixture (4626 data point) including 11 different cation-family (BuPy, C_2mim, C_3mim, C_4mim, C_6mim, C_8mim, Hmim, Mmim, Moim, OcPy and Omim) in the wide range of temperature, IL mole fraction and in the atmospheric pressure is modeled using two methods, i.e. cubic equations of state (Soave-Redlich-Kwong (SRK) EoS as two-parameter CEoS and Patel-Teja (PT) EoS as three-parameter CEoS) and six semi-empirical equations. The semi-empirical equations had fitting parameters and the they were obtained for each cation-family, separately. To obtain the fitting parameters of semi-empirical equations, the improved laplacian whale optimization algorithm (LXWOA) was applied.

2. Materials and methods

2.1. Data set

The values of molecular weight (M_w), critical molar volume (V_c), acentric factor (ω), critical pressure (P_c) and critical temperature (T_c) for each IL and solvent and as model input variables are necessary. Consequently, the mentioned properties of 51 ILs and 41 solvents that are used in this investigation, are provided in Table 1. The ILs critical properties were from references (Bagheri and Mohebbi, 2017; Bagheri and Ghader, 2017; Sheikhi-Kouhsar et al., 2015; Valderrama et al., 2008) and the critical properties of solvents were from references (Danesh, 1998; Green and Southard, 2019).

To calculate the density of IL + solvent binary systems, the enormous data set that covers a wide range of temperature, mole fraction, solvent and IL was provided. This data set was applied to developed the suggested models, contains 4626 experimental data point in the temperature range of 278.15–353.15 K, IL mole fraction range of 0.0040–0.9854 and atmospheric pressure. The data set was collected from references (Mokhtarani et al., 2009; Wang et al., 2012; Rilo et al., 2009; Solanki et al., 2013; Bhagour et al., 2013; Bhattacharjee et al., 2012; Wang et al., 2011; Bhujrajh and Deenadayalu, 2007; Quijada-Maldonado et al., 2012; Rodriguez and Brennecke, 2006; Wang et al., 2011; Zhao et al., 2012; Vercher et al., 2007; Sadeghi et al., 2009; Tong et al., 2009; Iglesias-Otero et al., 2008; Gao et al., 2009; Patel et al., 2016; Domańska et al., 2006; Kumar et al., 2012; Mokhtarani et al., 2008; Matkowska and Hofman, 2013;

Table 1 The thermodynamics features of ILs and solvents.

No.	Substance	M_w	T_c (K)	P_c (bar)	V_c (cm^3/mol)	Z_c	ω	Reference
1	[BuPy][BF$_4$]	223.019	597.600	20.30	648.1000	0.2682	0.8307	11
2	[BuPy][NO$_3$]	198.225	815.890	26.59	639.0367	0.2537	0.5981	15
3	[C$_2$mim][BF$_4$]	197.970	585.300	23.60	557.8230	0.2740	0.7685	15
4	[C$_2$mim][C$_2$SO$_4$]	236.300	968.100	40.40	676.8000	0.3441	0.8142	15
5	[C$_2$mim][CH$_3$SO$_4$]	222.268	1053.610	45.91	602.6700	0.3200	0.3400	15
6	[C$_2$mim][CH$_3$(OCH$_2$CH$_2$)$_2$OSO$_3$]	310.000	1162.900	28.10	862.3000	0.2539	0.5176	15
7	[C$_2$mim][DCA]	177.210	999.000	29.10	597.8000	0.2122	0.7661	15
8	[C$_2$mim][EtSO$_4$]	236.290	1061.100	40.40	578.6822	0.2684	0.3368	11
9	[C$_2$mim][[L-lactate]	200.241	965.989	26.32	620.1200	0.2059	0.9467	15
10	[C$_2$mim][NO$_3$]	173.174	918.398	33.30	531.68	0.2349	0.5678	39
11	[C$_2$mim][OAc]	170.210	807.100	29.20	544.0000	0.2398	0.5889	15
12	[C$_2$mim][OTf]	260.200	898.800	35.80	653.4000	0.3171	0.7509	59
13	[C$_2$mim][TFA]	224.200	824.670	28.86	593.4675	0.2530	0.6808	59
14	[C$_2$mim][triflate]	260.200	992.300	35.80	636.3977	0.2797	0.3255	59
15	[C$_3$mim][Br]	205.099	815.601	32.97	526.1600	0.2591	0.4505	15
16	[C$_3$mim][Glu]	200.263	992.821	26.41	765.56	0.2481	1.0174	11
17	[C$_4$mim][BF$_4$]	226.020	632.300	20.40	671.9651	0.2641	0.8489	15
18	[C$_4$mim][CH$_3$SO$_4$]	250.000	1081.600	36.10	716.9000	0.2915	0.4111	11
19	[C$_4$mim][Cl]	175.000	789.000	27.80	568.8000	0.2442	0.4908	11
20	[C$_4$mim][ClO$_4$]	238.669	722.540	22.64	716.5103	0.2735	0.8418	15
21	[C$_4$mim][EtSO$_4$]	264.349	1096.084	32.55	774.0000	0.2801	0.4497	15
22	[C$_4$mim][Glu]	286.354	1231.847	20.32	892.4346	0.1793	1.4083	15
23	[C$_4$mim][Gly]	214.290	1012.794	24.29	701.7463	0.2050	1.0513	15
24	[C$_4$mim][HSO$_4$]	236.300	1103.800	43.40	664.9000	0.3185	0.7034	59
25	[C$_4$mim][L-lactate]	228.295	1005.090	24.60	734.3400	0.2190	1.0172	59
26	[C$_4$mim][MeSO$_4$]	250.320	1081.600	36.10	643.4045	0.2616	0.4111	59
27	[C$_4$mim][OcSO$_4$]	349.000	1189.800	20.20	1116.7000	0.2310	0.7042	11
28	[C$_4$mim][PF$_6$]	284.180	708.900	17.30	779.4230	0.2317	0.7553	15
29	[C$_6$mim][BF$_4$]	254.070	690.000	17.90	772.7525	0.2442	0.9625	15
30	[C$_6$mim][Br]	247.200	841.100	26.70	728.4475	0.2817	0.6070	39
31	[C$_6$mim][Cl]	202.720	829.200	23.50	683.0308	0.2358	0.5725	39
32	[C$_6$mim][EtSO$_4$]	292.403	1125.917	27.14	888.2200	0.2609	0.5314	11
33	[C$_6$mim][MeSO$_4$]	278.376	1110.838	29.61	831.1100	0.2699	0.4899	59
34	[C$_6$mim][PF$_6$]	312.200	754.300	15.50	848.1796	0.2123	0.8352	59
35	[C$_8$mim][BF$_4$]	282.100	727.400	15.78	884.3653	0.2337	0.9956	59
36	[C$_8$mim][Br]	275.23	746.554	30.92	846.2769	0.4271	0.8065	59
37	[C$_8$mim][Cl]	230.780	869.400	20.30	797.0536	0.2267	0.6566	15
38	[C$_8$mim][C$_1$OSO$_3$]	250.310	1081.600	36.10	716.9000	0.2915	0.4111	15
39	[C$_8$mim][PF$_6$]	340.000	810.800	14.00	990.8609	0.2084	0.9385	15
40	[Hmim][BF$_4$]	254.000	706.300	17.90	786.2000	0.2428	0.6221	15
41	[Hmim][FAP]	612.298	861.545	88.70	1385.0400	1.7377	0.9062	15
42	[Hmim][PF$_6$]	312.230	764.900	15.50	893.7091	0.2206	0.8697	15
43	[Hmim][NTf$_2$]	447.420	1287.300	22.20	929.7630	0.1953	1.3270	39
44	[Mmim][CH$_3$SO$_4$]	208.000	1040.000	52.90	610.1200	0.3781	0.3086	11
45	[Mmim][MeSO$_4$]	208.240	1040.000	52.90	448.8029	0.2781	0.3086	11
46	[Moim][BF$_4$]	282.140	737.000	16.00	883.4000	0.2337	1.0287	11
47	[Moim][CH$_3$(OCH$_2$CH$_2$)$_2$OSO$_3$]	394.538	1257.282	18.44	1204.9900	0.2153	0.7786	59
48	[OcPy][BF$_4$]	279.133	692.340	15.99	876.5600	0.2467	0.9795	59
49	[OcPy][NO$_3$]	254.332	986.900	20.05	856.2795	0.2119	0.7495	59
50	[Omim][BF$_4$]	282.100	726.100	16.00	822.2359	0.2207	0.9954	59
51	[Omim][PF$_6$]	340.260	810.800	14.00	1007.4940	0.2119	0.9385	59
52	Acetone	58.080	508.200	47.01	206.6908	0.2329	0.3070	60
53	Acetonitrile	41.053	545.000	48.30	170.3680	0.1839	0.3380	61
54	Amino acid	200.900	710.350	19.19	743.3000	0.2447	0.5425	61
55	Benzaldehyde	106.120	694.750	46.50	335.5608	0.2736	0.3050	61
56	Benzyl alcohol	108.138	720.150	43.74	335.4608	0.2482	0.3631	61
57	Butanone	72.110	536.750	42.10	266.5694	0.2547	0.3200	61
58	Butyl acetate	116.158	575.400	30.90	383.5359	0.2509	0.4394	60
59	Butyl amine	73.140	531.950	42.00	290.0000	0.2790	0.3290	60
60	DEGMME [1]	120.150	630.050	35.40	366.8700	0.2511	0.8707	60
61	Dichloromethane	84.932	510.000	60.80	182.4035	0.2649	0.1986	60
62	Diethyl carbonate	118.100	576.050	33.90	356.1248	0.2553	0.4848	60
63	Di-EGMEE	134.180	602.050	28.60	421.9985	0.2442	0.5748	61

Table 1 (*continued*)

No.	Substance	M_w	T_c (K)	P_c (bar)	V_c (cm^3/mol)	Z_c	ω	Reference
64	Dimethyl carbonate	90.330	529.950	31.38	374.5837	0.2702	0.2711	61
65	Dimethyl sulfoxide	78.139	729.000	56.50	227.0000	0.2143	0.2806	61
66	EGMEE [2]	91.020	567.050	42.30	293.9262	0.2671	0.7591	61
67	EGMME [3]	76.100	562.050	50.10	241.9265	0.2627	0.7311	61
68	Ethanol	46.069	513.900	61.48	164.6178	0.2399	0.6450	60
69	Ethyl acetate	88.106	523.300	38.80	282.2150	0.2549	0.3660	60
70	Ethylene glycol	62.068	720.000	82.00	191.0000	0.2650	0.5068	60
71	Iso-butanol	58.140	408.100	36.48	262.7000	0.2861	0.1810	60
72	Methanol	32.042	512.600	80.97	116.3652	0.2239	0.5640	60
73	Methyl acetate	74.079	506.600	47.50	224.9187	0.2569	0.3310	60
74	Methyl methacrylate	100.116	566.000	36.80	319.3081	0.2529	0.2802	60
75	Pentanone	86.132	560.950	37.40	292.9209	0.2379	0.3448	61
76	PGMEE [4]	104.150	554.127	45.32	294.0736	0.2930	0.7238	61
77	PGMME [5]	90.140	553.050	43.40	293.9384	0.2810	0.7219	61
78	Pyridine	79.100	620.050	56.20	246.7049	0.2724	0.2430	61
79	Nitromethane	61.040	588.200	63.10	173.0000	0.2261	0.3480	61
80	MDEA [6]	119.630	677.050	37.00	313.3000	0.2086	0.9970	61
81	β-Pyridine	93.129	645.050	46.50	311.0000	0.2732	0.2706	61
82	1-Butanol	74.123	535.900	41.88	273.0054	0.2599	0.5692	61
83	1-Decanol	158.281	688.000	23.08	645.0000	0.2636	0.6070	61
84	1,3-Dichloropropane	112.980	560.000	42.40	291.0000	0.2684	0.2564	61
85	1,4-Dioxane	88.110	587.000	52.08	234.9209	0.2539	0.2793	61
86	1-Hexanol	102.175	611.300	34.46	377.0160	0.2589	0.5586	61
87	1-Octanol	130.228	652.300	27.83	509.0000	0.2646	0.5697	60
88	1-Propanol	60.096	536.800	51.69	216.4515	0.2539	0.6209	60
89	2-Propanol	60.096	508.300	47.65	217.0849	0.2479	0.6544	60
90	Tetrahedrofuran	72.110	504.200	51.90	224.0000	0.2809	0.2254	61
91	Tri-EGMEE	178.240	679.120	24.80	567.1593	0.2523	1.0590	61
92	Water	18.015	647.100	220.50	55.1466	0.2289	0.3450	60

[1] Diethylene glycol monomethyl ether.
[2] Ethylene glycol monoethyl ether.
[3] Ethylene glycol monomethyl ether.
[4] Propylene glycol monoethyl ether.
[5] Propylene glycol monomethyl ether
[6] N-methyldiethanolamine.

Gao et al., 2010; Jiang et al., 2013; Singh et al., 2013; Pau and Panda, 2012; Wandschneider et al., 2008; Zhong et al., 2007; Fan et al., 2009; Pal and Kumar, 2011; Pal et al., 2010; Kermanpour and Sharifi, 2012; Kermanpour, 2012; Kermanpour and Niakan, 2012; Pal and Kumar, 2012; Zhu et al., 2011; Gomez et al., 2006; Malek et al., 2014; Ijardar and Malek, 2014; Akbar and Murugesan, 2013; Akbar et al., 2016; González et al., 2012; Pereiro et al., 2006; Pereiro and Rodriguez, 2007; Jiang et al., 2012) and the more details are prepared in Table 2. The provided data set contains several chemical compounds (51 ILs and 41 solvents) and 130 binary systems. Also, ILs are counting 11 various cations and 25 various anions.

2.2. Equation of state

In 1873 van der Waals presented the first modification of ideal gas EoS by including in attraction and repulsive intermolecular forces (Bagheri et al., 2018; Soave, 1984). After that, many modifications have been presented to improve the van der Waals EoS by change in attraction and repulsive intermolecular forces to predict phase equilibrium behavior and thermody-

namic properties. For instance, Redlich and Kwong (Redlich and Kwong, 1949) modified van der Waals EoS attractive term, Soave (Soave, 1972; Soave et al., 1993) modified the temperature dependency of the Redlich and Kwong EoS and Peng and Robinson (Peng and Robinson, 1976) modified the attractive term. The mentioned cubic EoS are known as two-parameter EoS. The two-parameter EoSs predict the same critical compressibility factor for all components, but for example, critical compressibility factor for hydrocarbons component are in the of range 0.2–0.3. Also, in many cases the accuracy of two-parameter EoSs to calculate density and vapor pressure of components is unacceptable consequently, using of third parameter to modify the attractive term was supposed (Gaffney et al., 2018; Bagheri et al., 2019; Yang et al., 2018; Yokozeki and Shiflett, 2010; Bagheri et al., 2019; Kumar and Upadhyay, 2021). For example, Schmidt and Wenzel EoS (Schmidt and Wenzel, 1980) and Patel-Teja EoS (Patel and Teja, 1982) are two well-known three-parameter cubic EoSs. They used acentric factor (ω) as the third parameter.

The pressure explicit Patel-Teja (PT) EoS is as following (Bagheri and Mohebbi, 2017; Danesh, 1998; Patel and Teja, 1982):

Table 2 The ionic liquid + solvent mixtures investigated in this study.

No.	System	T (K)	x_{IL}	ND*	Reference
1	BuPyBF$_4$ + water	283.15–343.15	0.1440–0.8900	104	62
2	BuPyNO$_3$ + water	298.15	0.0091–0.9018	16	63
3	C$_2$mimBF$_4$ + water	298.15	0.0040–0.7774	17	64
4	C$_2$mimBF$_4$ + pridine	293.15–308.15	0.1225–0.9349	72	65
5	C$_2$mimBF$_4$ + β-pyridine	293.15–308.15	0.1217–0.9317	72	65
6	C$_2$mimBF$_4$ + acetone	293.15–308.15	0.1214–0.9203	72	66
7	C$_2$mimBF$_4$ + dimethylsulphoxide	293.15–308.15	0.1319–0.9249	72	66
8	C$_2$mimC$_2$SO$_4$ + water	283.15–343.15	0.1017–0.9977	49	67
9	C$_2$mimCH$_3$SO$_4$ + methanol	298.15	0.0500–0.9389	12	68
10	C$_2$mimCH$_3$(OCH$_2$CH$_2$)$_2$OSO$_3$ + methanol	298.15–313.15	0.0380–0.9830	45	69
11	C$_2$mimCH$_3$(OCH$_2$CH$_2$)$_2$OSO$_3$ + water	298.15–313.15	0.1110–0.9780	45	69
12	C$_2$mimDCA + water	298.15–343.15	0.0992–0.9067	40	70
13	C$_2$mimDCA + ethanol	298.15–343.15	0.1059–0.8666	40	70
14	C$_2$mimEtSO$_4$ + water	278.15–348.15	0.0084–0.7888	64	71
15	C$_2$mimL-lactate + water	298.15	0.0059–0.9390	17	72
16	C$_2$mimNO$_3$ + ethanol	298.15	0.0995–0.9000	9	73
17	C$_2$mimNO$_3$ + methanol	298.15	0.1000–0.8995	9	73
18	C$_2$mimOAc + water	298.15–343.15	0.0992–0.9067	40	70
19	C$_2$mimOAc + ethanol	298.15–343.15	0.1059–0.8666	40	70
20	C$_2$mimOTf + water	278.15–348.15	0.0076–0.7705	64	71
21	C$_2$mimTFA + water	278.15–348.15	0.0088–0.7950	64	71
22	C$_2$mimtriflate + methanol	278.15–318.15	0.0505–0.9489	65	74
23	C$_2$mimtriflate + water	278.15–338.15	0.0178–0.9498	133	74
24	C$_3$mimBr + acetonitrile	288.15–308.15	0.01578–0.9782	60	75
25	C$_3$mimBr + dimethyl sulfoxide	288.15–308.15	0.02769–0.9854	55	75
26	C$_3$mimGlu + amino acid	283.15–338.15	0.0390–0.5427	216	76
27	C$_4$mimBF$_4$ + ethanol	298.15	0.0517–0.8295	11	77
28	C$_4$mimBF$_4$ + nitromethane	298.15	0.0512–0.8634	13	77
29	C$_4$mimBF$_4$ + 1,3-dichloropropane	298.15	0.0536–0.9028	15	77
30	C$_4$mimBF$_4$ + ethylene glycol	298.15	0.0517–0.9083	14	77
31	C$_4$mimBF$_4$ + water	298.15	0.0017–0.9005	27	64
32	C$_4$mimBF$_4$ + ethanol	298.15	0.0986–0.9059	12	64
33	C$_4$mimBF$_4$ + benzaldehyde	298.15–313.15	0.1000–0.8990	36	78
34	C$_4$mimBr + ethylene glycol	293.15–323.15	0.0969–0.897	63	79
35	C$_4$mimCH$_3$SO$_4$ + 1-butanol	298.15	0.0745–0.9622	10	80
36	C$_4$mimCH$_3$SO$_4$ + 1-decanol	298.15	0.0603–0.9569	10	80
37	C$_4$mimCH$_3$SO$_4$ + 1-hexanol	298.15	0.0602–0.9714	10	80
38	C$_4$mimCH$_3$SO$_4$ + 1-octanol	298.15	0.0497–0.9605	10	80
39	C$_4$mimCH$_3$SO$_4$ + ethanol	298.15	0.0713–0.9614	10	80
40	C$_4$mimCH$_3$SO$_4$ + methanol	298.15	0.0507–0.9308	10	80
41	C$_4$mimCH$_3$SO$_4$ + water	298.15	0.0498–0.9783	12	80
42	C$_4$mimCl + ethylene glycol	298.15–318.15	0.0132–0.9126	36	81
43	C$_4$mimClO$_4$ + ethanol	283.15–343.15	0.1400–0.9000	71	82
44	C$_4$mimEtSO$_4$ + ethanol	283.15–328.15	0.0495–0.9020	32	83
45	C$_4$mimEtSO$_4$ + methanol	283.15–328.15	0.0501–0.8485	32	83
46	C$_4$mimGlu + benzylalcohol	298.15–313.15	0.1001–0.9001	36	84
47	C$_4$mimGly + benzylalcohol	298.15–313.15	0.1000–0.9000	36	84
48	C$_4$mimHSO$_4$ + water	303.15–343.15	0.1012–0.9917	35	67
49	C$_4$mimL-lactate + 1-butanol	298.15–318.15	0.1000–0.8997	27	85
50	C$_4$mimL-lactate + ethanol	298.15–318.15	0.0992–0.8974	27	85
51	C$_4$mimL-lactate + methanol	298.15–318.15	0.0997–0.8981	27	85
52	C$_4$mimL-lactate + water	298.15–318.15	0.1002–0.9010	27	85
53	C$_4$mimMeSO$_4$ + methanol	298.15–313.15	0. 0422–0.9526	44	86
54	C$_4$mimMeSO$_4$ + 1-propanol	298.15–313.15	0.0482–0.9510	44	86
55	C$_4$mimMeSO$_4$ + 2-propanol	298.15–313.15	0.0482–0.9531	40	86
56	C$_4$mimMeSO$_4$ + 1-butanol	298.15–313.15	0.0425–0.7996	32	86
57	C$_4$mimMS + water	298.15–323.15	0.2000–0.8000	30	87
58	C$_4$mimNTf$_2$ + 1-butanol	298.15	0.0941–0.8986	11	88
59	C$_4$mimNTf$_2$ + 1-propanol	298.15	0.0941–0.8986	10	88
60	C$_4$mimOcSO$_4$ + 1-butanol	298.15	0.0798–0.9450	10	80
61	C$_4$mimOcSO$_4$ + 1-hexanol	298.15	0.0999–0.8672	9	80
62	C$_4$mimOcSO$_4$ + 1-octanol	298.15	0.2472–0.9508	8	80
63	C$_4$mimOcSO$_4$ + 1-decanol	298.15	0.0627–0.9723	10	80

Table 2 (*continued*)

No.	System	T (K)	x_{IL}	ND*	Reference
64	$C_4mimOcSO_4$ + methanol	298.15	0.0088–0.9080	10	80
65	C_4mimPF_6 + benzaldehyde	298.15–313.15	0.0523–0.8996	40	89
66	C_4mimPF_6 + methyl methacrylate	283.15–353.15	0.0993–0.9014	117	90
67	C_4mimPF_6 + EGMEE	288.15–318.15	0.0507–0.8949	70	91
68	C_4mimPF_6 + di-EGMEE	288.15–318.15	0.0523–0.9059	70	91
69	C_4mimPF_6 + tri-EGMEE	288.15–318.15	0.0558–0.9075	70	91
70	C_4mimPF_6 + PGMME	288.15–308.15	0.0553–0.9574	24	92
71	C_4mimPF_6 + PGMME	288.15–308.15	0.0526–0.9468	24	92
72	C_4mimPF_6 + DEGMME	288.15–308.15	0.0864–0.8992	24	92
73	C_6mimBF_4 + 1-propanol	293.15–333.15	0.1006–0.8894	35	93
74	C_6minBF_4 + 2-propanol	293.15–333.15	0.0835–0.8507	45	94
75	C_6mimBF_4 + isobutanol	303.15–338.15	0.0536–0.8908	72	95
76	C_6mimBF_4 + EGMME	288.15–318.15	0.0530–0.9099	72	96
77	C_6mimBF_4 + butanone	298.15	0.0492–0.8931	13	97
78	C_6minBF_4 + butylamine	298.15	0.0492–0.8787	13	97
79	C_6mimBF_4 + ethylacetate	298.15	0.0498–0.8908	13	97
80	C_6mimBF_4 + tetrahedrofuran	298.15	0.0498–0.8925	13	97
81	C_6mimBr + EGMME	288.15–318.15	0.0541–0.9050	70	96
82	C_6mimCl + water	298.15–343.15	0.0583–0.8726	32	98
83	$C_6mimEtSO_4$ + ethanol	293.15–333.15	0.0554–0.8533	32	83
84	$C_6mimEtSO_4$ + methanol	283.15–328.15	0.0520–0.9139	32	83
85	$C_6mimMeSO_4$ + ethanol	293.15–333.15	0.0503–0.7699	32	83
86	$C_6mimMeSO_4$ + methanol	283.15–328.15	0.0612–0.9285	32	83
87	C_6mimPF_6 + EGMME	288.15–318.15	0.0503–0.9094	72	96
88	C_6mimPF_6 + butylacetate	293.15–323.15	0.0956–0.9354	70	99
89	C_6mimPF_6 + ethylacetate	293.15–323.15	0.0905–0.9560	70	99
90	C_8mimBF_4 + 1,4 dioxane	298.15–318.15	0.0859–0.8893	27	100
91	C_8mimBF_4 + tetrahedrofuran	298.15–318.15	0.0963–0.8612	27	100
92	C_8mimBr + ethylene glycol	293.15–323.15	0.1023–0.8983	63	79
93	C_8mimCl + ethylene glycol	298.15–318.15	0.0077–0.9583	36	81
94	C_8mimCl + water	298.15–343.15	0.0365–0.8516	36	98
95	$C_8mimC_1OSO_3$ + ethylene glycol	298.15–318.15	0.0052–0.9244	36	81
96	C_8mimPF_6 + butylacetate	293.15–323.15	0.1078–0.8946	63	99
97	C_8mimPF_6 + ethylacetate	293.15–323.15	0.1056–0.8895	63	99
98	$HmimBF_4$ + ethanol	298.15	0.0980–0.9000	9	64
99	$HmimBF_4$ + water	298.15	0.3032–0.9002	7	64
100	$HmimBF_4$ + N-methyldiethanolamine	303.15–323.15	0.1176–0.9030	55	101
101	$HmimFAP$ + N-methyldiethanolamine	303.15–328.15	0.1007–0.8993	54	102
102	$HmimNTf_2$ + 1-propanol	298.15–328.15	0.0578–0.9594	33	103
103	$HmimNTf_2$ + 2-propanol	298.15–328.15	0.0527–0.9379	33	103
104	$HmimNTf_2$ + acetone	288.15–298.15	0.0528–0.9483	33	103
105	$HmimNTf_2$ + acetonitrile	298.15–328.15	0.0503–0.9247	33	103
106	$HmimNTf_2$ + ethanol	298.15–328.15	0.0518–0.9351	36	103
107	$HmimNTf_2$ + dichloromethane	288.15–298.15	0.0570–0.9699	33	103
108	$HmimNTf_2$ + methanol	298.15–313.15	0.0198–0.9462	24	103
109	$HmimPF_6$ + acetone	298.15	0.0462–0.9518	12	104
110	$HmimPF_6$ + butanone	298.15	0.0579–0.9483	11	104
111	$HmimPF_6$ + diethyl carbonate	298.15	0.0098–0.9498	12	104
112	$HmimPF_6$ + dimethyl carbonate	298.15	0.0524–0.9500	11	104
113	$HmimPF_6$ + ethanol	293.15–303.15	0.0198–0.9920	34	105
114	$HmimPF_6$ + butylacetate	298.15	0.0365–0.9496	11	104
115	$HmimPF_6$ + ethylacetate	298.15	0.0585–0.9477	11	104
116	$HmimPF_6$ + methylacetate	298.15	0.0411–0.9499	11	104
117	$HmimPF_6$ + pentanone	298.15	0.0538–0.9519	11	104
118	$MmimCH_3SO_4$ + 1-butanol	298.15	0.0583–0.9698	12	80
119	$MmimCH_3SO_4$ + ethanol	298.15	0.0511–0.9551	11	80
120	$MmimCH_3SO_4$ + methanol	298.15	0.0660–0.9198	10	80
121	$MmimCH_3SO_4$ + water	298.15	0.0206–0.9376	14	80
122	$MmimMeSO_4$ + ethanol	293.15–303.15	0.0738–0.9512	33	105
123	$MoimBF_4$ + ethanol	298.15	0.1012–0.9014	9	64
124	$MoimCH_3(OCH_2CH_2)_2OSO_3$ + methanol	298.15–313.15	0.1100–0.9090	18	69
125	$OcPyBF_4$ + water	283.15–348.15	0.2170–0.9000	112	62
126	$OcPyNO_3$ + methanol	298.15	0.1026–0.9360	8	106

Table 2 (*continued*)

No.	System	T (K)	x_{IL}	ND*	Reference
127	OcPyNO$_3$ + ethanol	298.15	0.2000–0.8760	8	106
128	OcPyNO$_3$ + 1-butanol	298.15	0.1245–0.8990	8	106
129	OmimBF$_4$ + ethanol	283.15–343.15	0.2470–0.9190	78	82
130	OmimPF$_6$ + ethanol	293.15–303.15	0.0447–0.9502	33	105
	Total number of data			4626	

* Number of experimental data point.

$$P = \frac{RT}{v-b} - \frac{a_c a(T)}{v(v+b) + c(v-b)} \tag{1}$$

where R is the universal gas constant and v is the molar volume. Also, the parameters are as following (Bagheri and Mohebbi, 2017; Patel and Teja, 1982):

$$a_c = \left(\Omega_{aci} \frac{(RT_{ci})^2}{P_{ci}}\right)\alpha(T) \tag{2}$$

$$\alpha(T) = \left[1 + m_i\left(1 - \sqrt{\frac{T}{T_{ci}}}\right)\right]^2 \tag{3}$$

$$m_i = 0.452413 + 1.30982\omega_i - 0.295937\omega_i^2 \tag{4}$$

$$b_i = \Omega_{bi}\frac{RT_{ci}}{P_{ci}} \tag{5}$$

$$c_i = \Omega_{ci}\frac{RT_{ci}}{P_{ci}} \tag{6}$$

$$\Omega_{ci} = 1 - 3\eta_i \tag{7}$$

$$\eta_i = 0.329032 - 0.076799\omega_i + 0.0211947\omega_i^2 \tag{8}$$

$$\Omega_{bi}^3 + (2 - 3\eta_i)\Omega_{bi}^2 + 3\eta_i^2\Omega_{bi} - \eta_i^3 = 0 \tag{9}$$

$$\Omega_{aci} = 3\eta_i^2 + 3(1 - 2\eta_i)\Omega_{bi} + \Omega_{bi}^2 + (1 - 3\eta_i) \tag{10}$$

Furthermore, Patel-Teja EoS in the form of compressibility factor is as following (Bagheri and Mohebbi, 2017):

$$Z^3 + (C-1)Z^2 + (A - 2BC - B - C - B^2)Z$$
$$+ (BC + B^2C - AB) = 0 \tag{11}$$

The pressure explicit SRK EoS is as following (Danesh, 1998; Patel and Teja, 1982):

$$P = \frac{RT}{v-b} - \frac{a(T)}{v(v+b)} \tag{12}$$

Furthermore, the SRK EoS based on compressibility factor as follows (Danesh, 1998):

$$Z^3 - Z^2 + (A - B - B^2)Z + AB = 0 \tag{13}$$

The pure component parameters a_i and b_i are given by the following equations (Bagheri et al., 2018):

$$a_i = 0.42747\frac{R^2T_{ci}^2}{P_{ci}}\left[1 + m_i\left(1 - \sqrt{\frac{T}{T_{ci}}}\right)\right]^2 \tag{14}$$

$$b_i = 0.08664\frac{RT_{ci}}{P_{ci}} \tag{15}$$

$$m_i = 0.48 + 1.574\omega_i - 0.176\omega_i^2 \tag{16}$$

The coefficients a, b and c for mixtures are obtained from van der Waals type I mixing rule (Bagheri et al., 2018; Ghalandari et al., 2020):

$$a_m = \sum_i\sum_j x_i x_j \sqrt{a_i a_j}(1 - k_{ij}) \tag{17}$$

$$b_m = \sum_i x_i b_i \tag{18}$$

$$c_m = \sum_i x_i c_i \tag{19}$$

2.3. Semi-empirical equation

There is a great change of analytical expressions, which permit predicting and correlating the density of liquids. Such correlations are usually according to apply of adjustable parameters for each component (Geppert-Rybczyńska et al., 2010; Singh et al., 2014). But, the mentioned types of generalized correlations were not developed for IL-mixture systems. Several semi-empirical equations were presented to predict pure IL density. In this communication, through several presented semi-empirical equations, six semi-empirical equations were selected and the details are given as following (Elbro et al., 1991; Mchaweh et al., 2004; Gunn and Yamada, 1971; Hankinson and Thomson, 1979; Poling et al., 2001; Sandler, 2017; Kontogeorgis and Folas, 2009 Dec 1):

$$\ln\frac{M_w P_c}{R\rho T} = \ln V^0 + \omega \ln V^1$$

$$\ln V^0 = a_0 + a_1 T_r + a_2 T_r^2 + a_3 T_r^3 + a_4 T_r^4 + a_5 T_r^5 + a_6 T_r^6$$

$$\ln V^1 = b_0 + b_1 T_r + b_2 T_r^2 + b_3 T_r^3 + b_4 T_r^4 + b_5 T_r^5 + b_6 T_r^6 \tag{20}$$

$$\rho = \frac{M_w}{V_c}\left(a_0 + a_1\tau^{\frac{1}{3}} + a_2\tau^{\frac{2}{3}} + a_3\tau + a_4\tau^{\frac{4}{3}}\right)$$

$$\tau = 1 - \frac{T_r}{\left[1 + (0.48 + 1.574\omega - 0.176\omega^2)(1 - \sqrt{T_r})\right]^2} \tag{21}$$

$$\rho = \frac{P_c M_w}{RT_c V_1(1 - \omega V_2)(a_0 + a_1\omega)}$$

$$0.2 < T_r < 0.8 : V_1 = b_0 + b_1 T_r + b_2 T_r^2 + b_3 T_r^3 + b_4 T_r^4$$

$$0.8 < T_r < 1 : V_1$$
$$= b_0 + b_1\sqrt{1 - T_r}\log(1 - T_r) + b_2(1 - T_r) + + b_3(1 - T_r)^2$$

$$V_2 = c_0 + c_1 T_r + c_2 T_r^2 \tag{22}$$

$$\rho = \frac{M_w}{V_c\left[V^0 + \left(1 - \frac{\omega\left(b_0 + b_1 T_r + b_2 T_r^2 + b_3 T_r^3\right)}{T_r + b_4}\right)\right]}$$

$$V^0 = a_0 + a_1(1 - T_r)^{\frac{1}{3}} + a_2(1 - T_r)^{\frac{2}{3}} + a_3(1 - T_r) + a_4(1 - T_r)^{\frac{4}{3}} \tag{23}$$

$$\rho = \left(\sum_i \frac{P_{ci}M_{wi}}{RT_{ci}x_i}\right)\left(a_0 + a_1\omega + a_2\omega^2 + a_3\omega^4\right)^{-\left(1 + (1 - T_r)^{\frac{2}{7}}\right)} \tag{24}$$

Also, the Nasrifar-Moshfeghian (NM) equation was used to predict the density of binary IL + solvent. The equation is expressed by (Nasrifar and Moshfeghian, 1998; Rabari et al., 2014; Mathias and Copeman, 1983):

$$\rho = \frac{M_w}{V_c}\rho_0\left[1 + \delta(f(T_r) - 1)^{\frac{1}{3}}\right] \tag{25}$$

$$\rho_0 = 1 + 1.1688\left(1 - \frac{T_r}{f(T_r)}\right)^{\frac{1}{3}} + 1.8177\left(1 - \frac{T_r}{f(T_r)}\right)^{\frac{2}{3}}$$
$$- 2.65811.1688\left(1 - \frac{T_r}{f(T_r)}\right) + 2.1613\left(1 - \frac{T_r}{f(T_r)}\right)^{\frac{4}{3}} \tag{26}$$

$$f(T_r) = \left[1 + c_0\left(1 - \sqrt{T_r}\right) + c_1\left(1 - \sqrt{T_r}\right)^2 + c_2\left(1 - \sqrt{T_r}\right)^3\right]^2, T_r < 1$$

$$f(T_r) = \left[1 + c_0\left(1 - \sqrt{T_r}\right)\right]^2, T_r > 1 \tag{27}$$

As mentioned, the presented semi-empirical equations, for first time, were used for pure liquids (except Eq. (24)). Subsequently, to develop them to IL-mixture systems the mixing rules must be applied. There are five thermodynamic properties in equations (20) - (27) i.e. acentric factor, critical temperature, critical pressure, critical volume and molecular weight. In this study, various mixing rules were considered. The details of all mixing rules and the final mixing rules that were applied, are provided in Table 3.

2.3.1. Pre-processing of the train and test

The AI learning approaches used to estimate the target parameters applying input parameters are widely nonlinear and depend mainly on the learning database (Memarzadeh et al., 2020; Ali et al., 2018; Nguyen-Huy et al., 2018). In cases where we are dealing with large-scale data processing, dimensionality reduction and subset selection methods can be necessary and useful tools in model development (Xu et al., 2019; Riahi-Madvar and Seifi, 2018). Important points that are essential in designing the precise prediction model for the AI model include the selection of appropriate input and data clustering techniques due to the diversity of the data set (Riahi-Madvar and Seifi, 2018; Loey et al., 2021; Mueller and Massaron, 2021). In order to achieve reliable data subsets for training and testing, the subset selection of maximum dissimilarity method (SSMD) was used to select training and testing subsets through a random manipulation of these data sets. Selecting the most appropriate train sets in the proposed preprocessing strategy is the most important task in SSMD-based approaches for data selection, which extremely depends on the expansion of the data (Riahi-Madvar and Seifi, 2018). In the SSMD method, data selection is not focused only on a specific area. Although these data are very different from each other, they can still show the statistical features of the original dataset (Lajiness and Watson, 2008). The data must first be normalized. Thus, the process of normalization and then de-normalization of the initial data set is performed by Eq. (28), respectively.

$$y_n = \frac{y_i - y_{min}}{y_{max} - y_{min}} \rightarrow y_i = y_n(y_{max} - y_{min}) + y_{min} \tag{28}$$

The Kennard-Stone (KS) algorithm is used to describe the SSMD in which a subset of N points in j dimensional space is selected (Kennard and Stone, 1969). The candidates of subset for training can be defined by the following matrix Y:

$$y = \begin{pmatrix} y_{11} & \cdots & y_{j1} \\ \vdots & \ddots & \vdots \\ y_{1N} & \cdots & y_{jN} \end{pmatrix} \tag{29}$$

where Y represents a data set as $Y = (y_1; y_2; \cdots; y_j)$ that contains j factor and a set of N points in j dimensional space defined by j factors (Kennard and Stone, 1969). The selection of design points is done sequentially (Riahi-Madvar et al., 2019). The goal in each step is to select points that are evenly

Table 3 The details of all mixing rules for thermodynamic properties (Poling et al., 2001; Sandler, 2017; Kontogeorgis and Folas, 2009 Dec 1; Nasrifar and Moshfeghian, 1998).

Property	Tested mixing rule	Final mixing rule
M_w	$M_w = \sum_i x_i M_{wi}$	$M_w = \sum_i x_i M_{wi}$
T_c	$T_c = \frac{T_{ci} + T_{cj}}{2}$ $T_c = \sum_i x_i T_{ci}$ $T_c = \sum_i\sum_j x_i x_j T_{cij}$, $T_{cij} = \sqrt{T_{ci}T_{cj}}$	$T_c = \sum_i\sum_j x_i x_j T_{cij}$
	$T_c = \frac{1}{\sum_i \frac{x_i}{T_{ci}}}$	
V_c	$V_c = \left(\frac{\sqrt[3]{V_{c1}} + \sqrt[3]{V_{c2}}}{2}\right)^3$ $V_c = \sum_i x_i V_{ci}$ $V_c = \sum_i\sum_j x_i x_j V_{cij}$, $V_{cij} = \left(\frac{\sqrt[3]{V_{c1}} + \sqrt[3]{V_{c2}}}{2}\right)^3$	$V_c = \sum_i x_i V_{ci}$
P_c	$P_c = \frac{P_{ci} + P_{cj}}{2}$ $P_c = \sum_i x_i P_{ci}$ $P_c = \frac{1}{\sum_i \frac{x_i}{P_{ci}}}$ $P_c = \sum_i\sum_j x_i x_j P_{cij}$, $P_{cij} = \sqrt{P_{ci}P_{cj}}$	$P_c = \sum_i x_i P_{ci}$
	$P_c = \frac{Z_{cij}RT_{cij}}{V_{cij}}, Z_{cij} = \frac{Z_{ci} + Z_{cj}}{2}, T_{cij} = \sqrt{T_{ci}T_{cj}}, V_{cij} = \left(\frac{\sqrt[3]{V_{c1}} + \sqrt[3]{V_{c2}}}{2}\right)^3$	
ω	$\omega = \frac{\omega_i + \omega_j}{2}$ $\omega = \sqrt{\omega_i\omega_j}$ $\omega = \sum_i x_i\omega_i$	$\omega = \sqrt{\omega_i\omega_j}$

spaced along the object area at each step of the algorithm. The first point is selected close to the average of the dataset and the second point is chosen so that it has the greatest distance from the first point. Eventually, the third point is selected so that it has the longest distance from the aforementioned two points. The training subcomponent involves these aspects of data points, in addition, the test subset includes the remaining data points (Wu et al., 1996). The subsets are selected by maximizing the minimum distance between the train dataset and the rest of the data points in the original dataset. The statistical features of the subsets obtained from the SSMD method are depicted in Table 4. As it can be seen from Table 4; all parameters have approximately the same distributions over train and test datasets, which is in accordance with the equal scale of standard deviation, kurtosis, skewness. Moreover, a wide range of ρ is observed from the longitudinal dispersion data in both training and testing stages.

2.3.2. LXWOA theories and formulation

To determine the coefficient of the semi-empirical equation using experimental data of IL-mixture, optimization algorithms must be used. Some of the algorithms that used to obtain the coefficients of semi-empirical equations are genetic algorithm, artificial bee colony algorithm, imperialist competitive algorithm, particle swarm optimization, and simulated

annealing (Singh, 2019). The whale optimization algorithm is a nature-inspired metaheuristic optimization algorithm, which is inspired by the search behavior of humpback whales. The main difference between LXWOA and WOA is the improved convergence of the algorithm. The LXWOA algorithm is a combination of the WOA and Laplace crossover algorithms, which was introduced by Singh for the first time (Singh, 2019). The whale optimization algorithm is a novel nature-inspired *meta*-heuristic optimization method, which was presented by Mirjalili and Lewia (Mirjalili and Lewis, 2016). The WOA method is inspired by the social behavior and the bubble-net hunting strategy of humpback whales in which the bubble-net hunting behavior is used to prey hunting. One of the advantages of the WOA method is that it does not need a large amount of initial information. This feature makes the method have a small number of adjustment parameters that can be easily tuned for a great variety of applications. The LXWOA algorithm consists of the following steps: In the first step, an initial population of size N_p is generated randomly from the data set. In the second step, the WOA method is first followed by the LXWOA in each iteration, then two agents are chosen (Singh, 2019). The best agent is determined by the first agent and the second agent is randomly chosen from the present population. In the third step, laplace crossover operators are used to create two offspring by combining the best and

Table 4 The summary statistics of the parameters in train, test and over all of the sets.

	Parameter	Mean	Mode	SD	Min	Median	Maximum	Skewness	Kurtosis
Total data set	ρ	1.110	1.0836	0.121	0.772	1.120	1.398	−0.481	3.000
	X_1	0.459	0.200	0.298	0.0009	0.406	0.997	0.220	1.739
	T	305.470	298.150	15.583	278.150	303.150	353.15	0.687	3.241
	M_{w1}	236.916	236.30	51.811	107.110	236.300	648.867	0.636	10.208
	T_{c1}	862.300	968.100	162.090	571.300	898.800	1376.1	0.054	1.759
	ω_1	0.712	0.8140	0.209	0.308	0.814	1.408	−0.226	2.264
	V_{c1}	689.000	676.80	146.162	298.240	676.800	1983.5	0.988	13.758
	M_{w2}	59.080	18.020	56.734	18.020	46.070	350	3.552	18.205
	T_{c2}	589.171	647.100	83.601	506.550	562.050	837.15	0.942	3.302
	ω_2	0.4997	0.345	0.178	0.198	0.564	1.106	0.477	2.667
	V_{c2}	195.260	55.900	186.530	55.900	1670	1175	3.790	20.000
Testing data set	ρ	1.1025	1.083	0.114	0.772	1.108	1.398	−0.350	3.131
	X_1	0.453	0.200	0.280	0.0009	0.409	0.997	0.213	1.852
	T	306.686	298.150	15.593	278.150	303.150	353.15	0.687	3.224
	M_{w1}	238.119	236.300	54.294	107.110	240.000	648.867	0.364	7.896
	T_{c1}	851.230	968.100	164.862	571.300	802.145	1376.100	0.280	1.777
	ω_1	0.7174	0.814	0.214	0.308	0.814	1.408	−0.142	2.258
	V_{c1}	696.919	676.800	154.383	298.240	701.300	1983.500	0.670	10.302
	M_{w2}	64.049	18.020	64.633	18.020	46.070	350.000	3.220	14.377
	T_{c2}	590.359	647.100	85.869	506.550	562.050	837.150	1.024	3.490
	ω_2	0.526	0.345	0.183	0.198	0.564	1.106	0.374	2.649
	V_{c2}	213.477	55.900	214.080	55.900	167.000	1175.000	3.356	15.254
Training data set	ρ	1.129	1.029	0.134	0.780	1.167	1.395	−0.796	2.989
	X_1	0.474	0.242	0.335	0.0009	0.400	0.990	0.187	1.481
	T	302.654	298.150	15.195	278.150	298.150	353.150	0.714	3.288
	M_{w1}	234.107	236.300	45.385	107.111	236.300	648.867	1.623	20.296
	T_{c1}	888.174	968.100	152.386	571.30	968.100	13761.000	−0.527	2.167
	ω_1	0.699	0.814	0.198	0.325	0.814	1.357	−0.501	2.153
	V_{c1}	670.528	676.800	122.960	298.24	676.800	1983.500	2.187	32.166
	M_{w2}	47.478	18.020	28.090	18.02	41.050	134.178	0.760	2.565
	T_{c2}	586.395	647.100	78.008	506.55	560.000	802.050	0.655	2.424
	ω_2	0.436	0.345	0.149	0.198	0.345	0.870	0.527	2.106
	V_{c2}	152.741	55.900	80.346	55.900	167.000	422.000	0.404	2.442

Note: The subscript 1 is related to IL and the subscript 2 is related to solvent.

randomly selected agents. The fitness of each offspring over the worst agent in the present population is evaluated one by one. If offspring has better fitness over the worst agent, it is then replaced by the worst particle. The best search agent is then updated and iteration is increased. Finally, this process is followed by the algorithm till termination criteria is satisfied (Liakos et al., 2018).

2.3.2.1. Whale optimization algorithm. Searching for a prey, encircling prey, and spiral bubble-net feeding maneuver are two main phases that are used by humpback whales to prey hunting. In the searching for a prey (the first phase), a random search is done to explore the prey depending on the position of each other (exploration phase). In the encircling prey and spiral bubble-net attacking (the second phase), the location of prey is perceived by the humpback whales after encircling them and the spiral updating position are implemented (exploitation phase). Since the optimal solution is not known in the a priori search space, the best current candidate solution is considered by the WOA algorithm as the target prey or close to the optimum target point. The WOA algorithm has received a lot of attention in recent years due to its advantages such as simple principle, simple operation, easy implementation, few adjustment parameters, and strong robustness, and many valuable research results have been obtained in this field. Moreover, the research results show that the WOA algorithm significantly outperformed other optimization algorithms, such as differential evolution and gravitational search in terms of solution accuracy and algorithm stability. Therefore, according to the above explanations, this algorithm was used in the present study. After the position of the best search agent is defined by the algorithm, the position of the other search agents will be updated towards the best search agent. The mathematical model of WOA is provided as follows: let N_P be the population size and M_{itr} be MaxIter (Mirjalili and Lewis, 2016; Liakos et al., 2018; Kotsiantis et al., 2006; Dutton and Conroy, 1997; Maxwell et al., 2018). The method consists of two adjustable parameters a and b, which the value of the parameter a linearly decreases in the range 2 to 0 through iterations and the value of the parameter b reduces from -1 to -2. Next, the coefficients A_i, C_i and a random number l_i are calculated for agent i by the following equations (Singh, 2019):

$$A_i = 2ar_1 - a, C_i = 2r_2, l_i = (b-1)r_3 + 1 \qquad (30)$$

where r_1, r_2 and r_3 represent three random numbers that are uniformly distributed on the interval from 0 to 1. Next, a random number p_r is generated in (0; 1). If $0.5 \geq p_r$ and $|A_i| \geq 1$, the dth particle of the next position ($x_i^d(t+1)$) is updated by the ith agent through the $x_{rand}^d(t)$ agent as follows (Singh, 2019):

$$D_i^d = \left| C_i x_{rand}^t(t) - x_i^d(t) \right|, x_i^d(t+1) = x_{rand}^d(t) - A_i D_i^d \qquad (31)$$

where $x_{rand}^d(t)$ indicates a random position of ith agent in d^{th} dimension at time t. Now, If $p_r < 0.5$ and $|A_i| < 1$, the dth particle of next position ($x_i^d(t+1)$) is updated by the ith agent through the x_{best}^d agent as follows (Singh, 2019):

$$D_i^d = \left| C_i x_{best}^t(t) - x_i^d(t) \right|, x_i^d(t+1) = x_{bset}^d(t) - A_i D_i^d \qquad (32)$$

Next, if $p_r \geq 0.5$ the following spiral model is generated by evaluating the distance between the whale postion (x_i) and prey postion (x_{best} (t)) in d^{th} dimension $D_i^d = \left| C_i x_{best}^t(t) - x_i^d(t) \right|$ at iteration t to imitate the helix-shaped movement of humpback whales (Singh, 2019):

$$x_i^d(t+1) = D_i^d e^{bl_i} \cos(2\pi l_i) + x_{bset}^d(t) \qquad (33)$$

The Laplace crossover (LX) is proposed by Deep and Thakur for the first time in which two off-springs i.e. $y_1 = (y_1^1, y_1^2, \cdots\cdots, y_1^m)$ and $y_2 = (y_2^1, y_2^2, \cdots\cdots, y_2^m)$ are generated from a pair of parents i.e. $x_1 = (x_1^1, x_1^2, \cdots\cdots, x_1^m)$ and $x_2 = (x_2^1, x_2^2, \cdots\cdots, x_2^m)$ in such a way that both of the off-spring have a symmetric position over the parents position. Next, two uniformly distributed random numbers u_i 2 [0; 1] and v_i 2 [0; 1] are firstly generated (Mirjalili and Lewis, 2016; Kotsiantis et al., 2006). Then, a random number l_i is generated by simply inverting the distribution function of Laplace distribution as follows:

$$l_i = \begin{cases} p - q\ln(u_i) v_i \leq 0.5 \\ p + q\ln(u_i) v_i > 0.5 \end{cases} \qquad (34)$$

where $p \in R$ and $q > 0$ are called the location parameter and the scale parameter, respectively.

The off-springs are generated as follows:

$$y_1^i = x_1^i + l_i \left| x_1^i - x_2^i \right|, y_1^i = x_2^i + l_i \left| x_1^i - x_2^i \right| \qquad (35)$$

If for some of i the created off-spring are outside the search space i.e. $y^i < y_{low}^i$ or $y^i > y_{up}^i$, a random number is then selected from $\left[y_{low}^i, y_{up}^i \right]$ for y^i as the generated off-spring. For smaller values of q, LX produces the off-spring close to the parents and for greater values of q; LX produces the off-springs away from the parents. For fixed values of p and q, LX dispenses off-springs according to the parents dispersion (Mirjalili and Lewis, 2016; Liakos et al., 2018). An equation for ρ is firstly defined based on previous literature to run the algorithm. The parameters obtained from the equation are then used as variables for the LXWOA algorithm. Moreover, a suitable objective function will be defined for the implementation of the algorithm in the following section. In this regards, at the end of each iteration, the best value of x_{best}^d must be found by the algorithm through changing the values of the variables. Eventually, the optimal solution rapidly converges towards a local optimum after a couple hundred times of running the algorithm. Eventually, after running the program a couple of hundred times, the convergence towards the optimal solution is achieved by the algorithm. This means that the hunting location has been identified and surrounded by the humpback whale. The flowchart of the implied algorithm is noticed in Fig. 1.

The main contribution of the proposed LXWOA algorithm is addressed in this subsection. After performing repeated runs of the optimization algorithm, it was found that it is not feasible to provide an equation that covers all the data. This creates some difficulty; first of all, the algorithm will not converge properly. The second problem is that the error value R_2 will increase because the algorithm has insisted on synchronizing and fitting itself overall data despite the high errors. Thus, a solution must be provided to prevent this problem at the various stages of the learning process. This means that one should try to converge the proposed model to less error data as much as possible. In this regard, the cumulative distribution function (CDF) function of the errors is defined as an objective function for the LXWOA optimization algorithm. Therefore, the objective function is considered as a coefficient ($\gamma = 0.8$) of CDF for the error defined as follows:
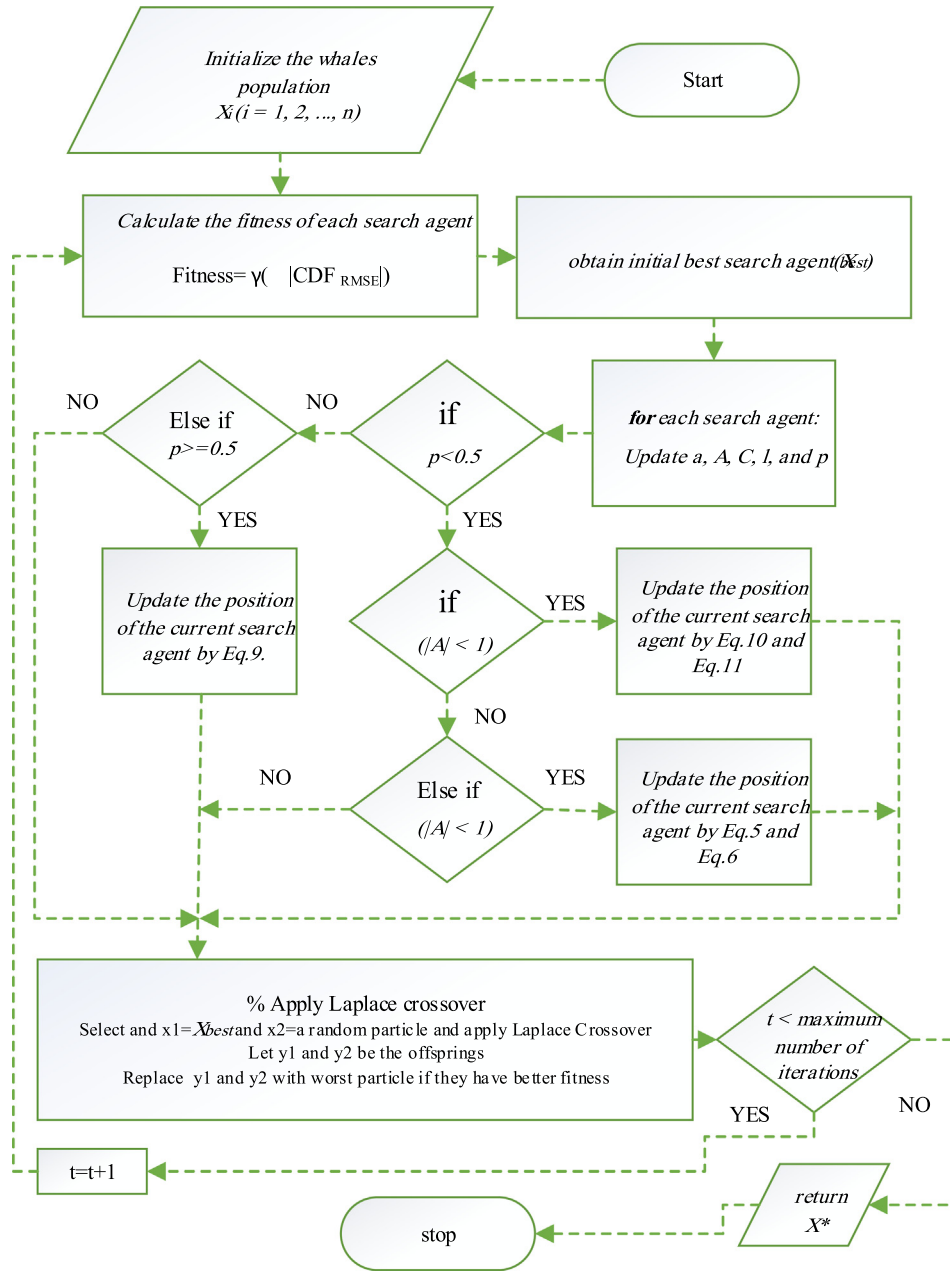
Fig. 1   The algorithm of LXWOA method.

$$Error(i) = y_{Predictedvalue}(i) - y_{Observedvalue}(i)$$

$$Fitness = \gamma\left(\sum |CDF_{errors}|\right) \qquad (36)$$

Indeed, some of the data generated by the LXWOA model may differ significantly from the actual data. Therefore, there is a lot of error in this data. This portion of the data may contain up to 10 to 20 percent of total data per run of the optimizer program. Therefore, if we want to present the cost function in the optimization algorithm in such a way that it puts pressure on all data to reduce the total error, it causes the model to move away from convergence in data with less error at the cost of achieving a lower error. In this regard, we try to reduce the model pressure on high errors each time the optimization process is performed. For this purpose, the

CDF of the errors is first obtained. Part of the errors (with a coefficient (0.8)) is then considered as a criterion for the cost function.

3. Results and discussion

No CEoS can prepare exact descriptions of behavior of real-fluid in all interest regions. Both SRK EoS and PT EoS consider only the attractive and repulsive intermolecular force between molecules. However, they have fundamental challenge to pure and mixture liquid density and the modification has been made to improve CEoS capability using modifying the repulsive and attractive terms (Sheikhi-Kouhsar et al., 2015). In this study, in the first step, the accuracy of SRK EoS and

PT EoS was investigated. For example, Fig. 2 indicates the density behavior of C_6mimBr + EGMME at x_{IL} = 0.3990 and x_{IL} = 0.7003 and C_6mimPF_6 + EGMME at x_{IL} = 0.2006 and x_{IL} = 0.8019 and at atmospheric pressure based on SRK EoS and PT EoS. Both CEoSs could not predict the mixture density with satisfactory accuracy. To decrease the deviation, the binary interaction parameter (k_{ij}) was used for both of them; however, the effect of interaction parameter on improving the modeling results was insignificant.

As another suggestion to model the IL-mixture density, application of semi-empirical equations was studied. The various semi-empirical equations were developed in this commu-nication (see Appendix A). The semi-empirical equation parameters are determined by matching prediction density (based on semi-empirical equation) with experimental data. To model the density of IL-mixture systems based on semi-empirical equations, two methods was considered. In the first method, the coefficients of Eqs. (20) - (24) that were presented by authors (Valderrama and Zarricuetac, 2009; Hosseini et al., 2013) with all mixing rules that are provided in Table 3, was applied. The obtained results indicated presented coefficients was not appropriate idea to predict IL-mixture systems. For instance, Fig. 3 indicates the results of $C_4mimHSO_4$ + water at x_{IL} = 0.2066 and $C_2mimC_2SO_4$ + water x_{IL} = 0.8775 using
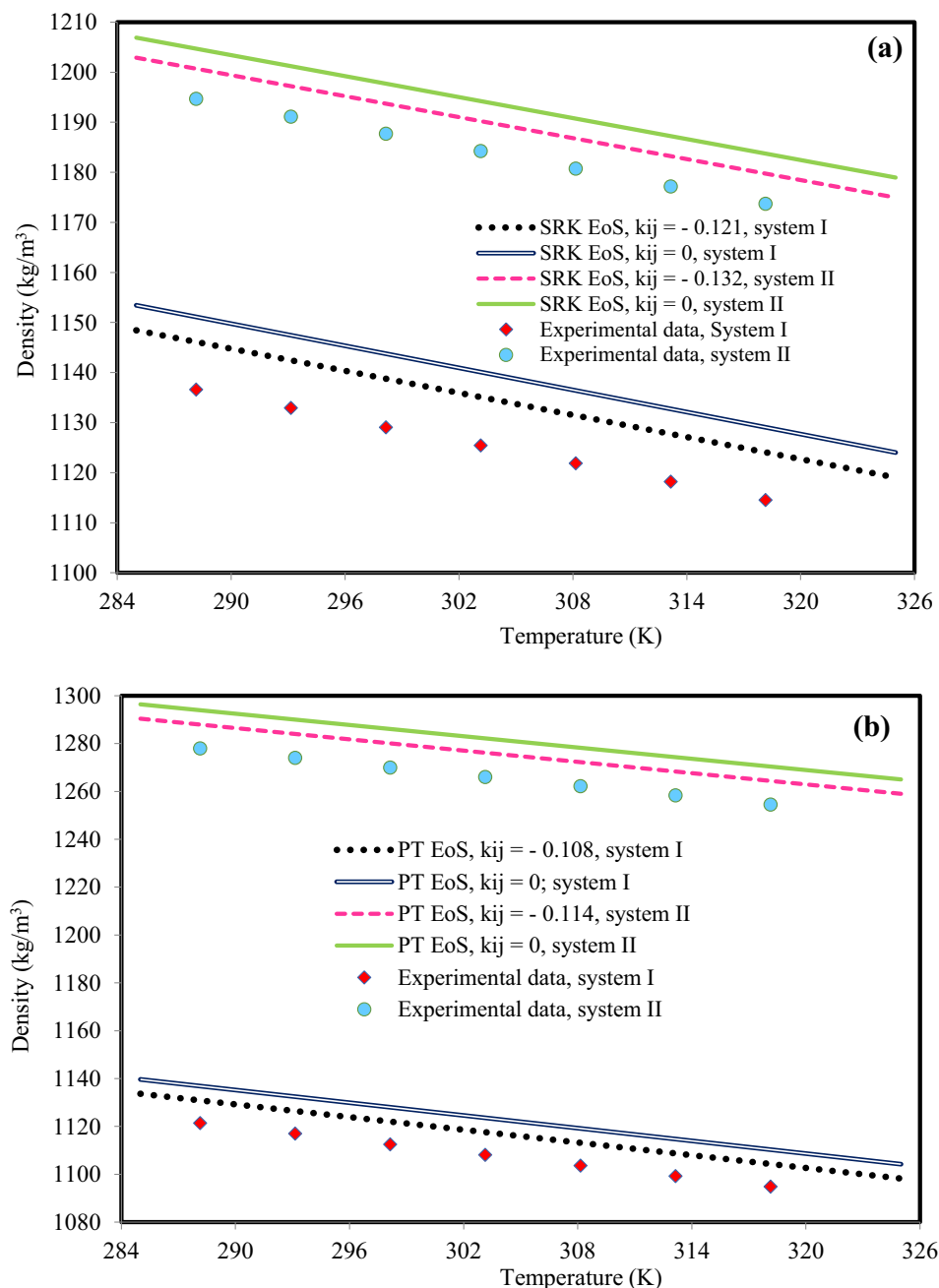
Fig. 2 The density behavior of (a) C_6mimBr + EGMME (system I: x_{IL} = 0.3990; system II: x_{IL} = 0.7003) and (b) C_6mimPF_6 + EGMME (system I: x_{IL} = 0.2006; system II: x_{IL} = 0.8019). The experimental data are from Pal and Kumar (Pal and Kumar, 2012).
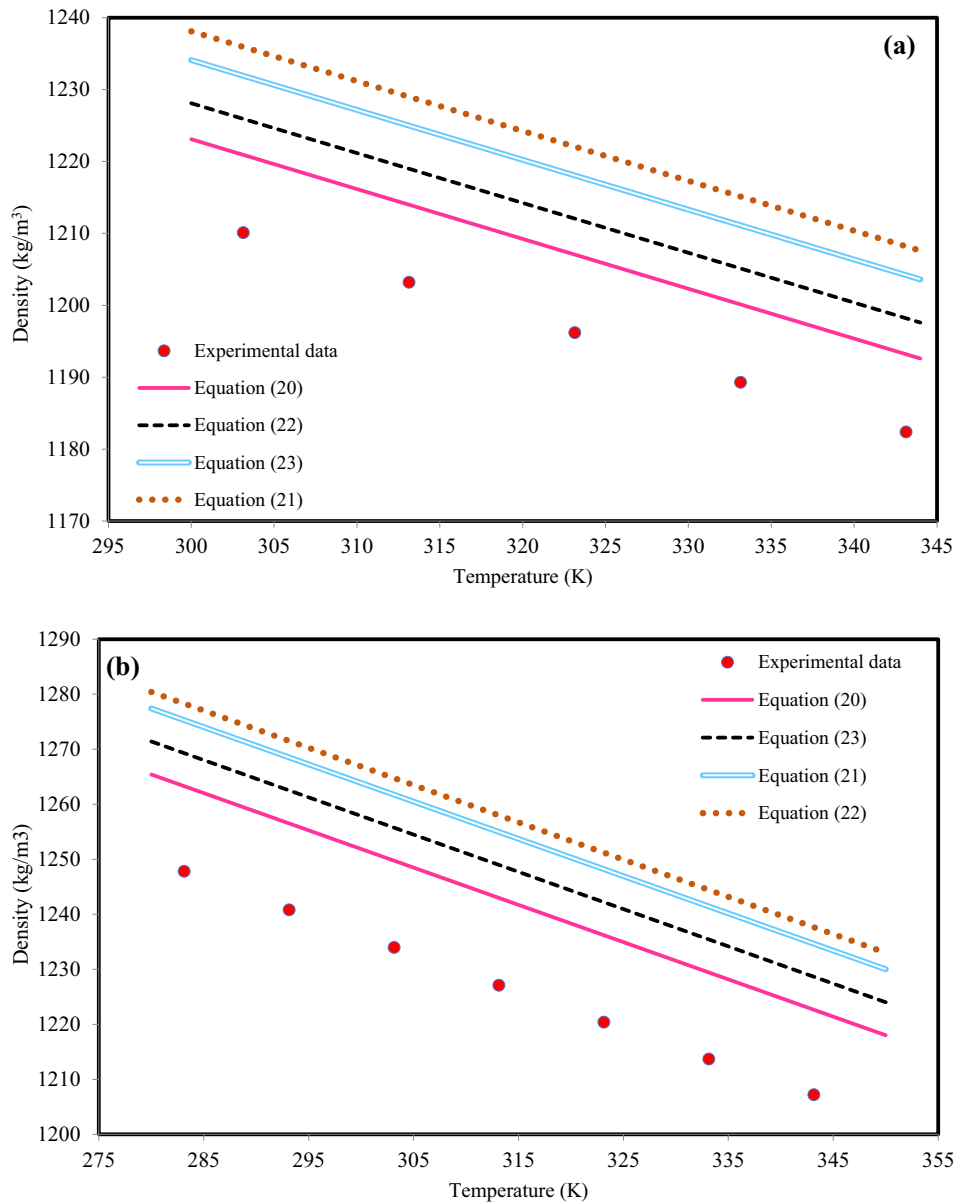
Fig. 3 The density behavior of (a) C$_4$mimHSO$_4$ + water, x$_{IL}$ = 0.2066 and (b) C$_2$mimC$_2$SO$_4$ + water, x$_{IL}$ = 0.8775. The experimental data are from Bhattacharjee et al. (Bhattacharjee et al., 2012).

Eqs. (20) - (24) with available coefficients in the literature (Valderrama and Zarricuetac, 2009; Hosseini et al., 2013). The behavior of all equations is out of experimental data. Indeed, this behavior was predictable. Due to the presented coefficients by authors (Valderrama and Zarricuetac, 2009; Hosseini et al., 2013) were obtained based on pure experimental data.

In the second method, the coefficients of Eqs. (20) - (25) was optimized using improved laplacian whale optimization algorithm. ILs composed of various cation structures and due to the behavior of each cation-family is similar, subsequently; to present a comprehensive IL-mixture density model, the semi-empirical equation coefficients of each cation-family were obtained, separately. In order, to obtain the coefficients, 70% of experimental data of each cation-family were used (according to SSMD method) and the rest of them were applied

to investigate the accuracy of presented modification. Table 5 indicates the obtained results of coefficients of each cation-family.

The statistical validation of optimized coefficients was investigated by introducing four statistical parameters of correlation factor (R^2), average absolute percent deviation (AAPD), standard deviation (STD) and root mean squared error (RMSE). These parameters are formulated as following and the values of them are provided in Table 6.

$$R^2 = 1 - \frac{\sum_{i=1}^{N} \left(\rho_{Calc.}(i) - \rho_{Exp.}(i) \right)^2}{\sum_{i=1}^{N} \left(\rho_{Calc.}(i) - \bar{\rho}_{Exp.}(i) \right)^2} \tag{37}$$

$$AAPD = \frac{1}{N} \sum_{i=1}^{N} \left| \frac{\rho_{Exp.} - \rho_{Calc.}}{\rho_{Exp.}} \right| \times 100 \tag{38}$$

Table 5 The optimization coefficients of semi-empirical equation based on cation-family.

	BuPy	C$_2$mim	C$_3$mim	C$_4$mim	C$_6$mim	C$_8$mim	Hmim	Mmim	Moim	OcPy	Omim
Eq. (20)											
a_0	1.4276	1.4333	3.4141	2.5435	1.5269	2.2006	1.2667	1.4437	2.6180	1.6672	1.4351
a_1	−24.4288	−12.1559	−16.3907	−20.5247	−18.5703	−25.5447	−22.8585	−19.3457	−17.1898	−27.4722	−25.7281
a_2	90.4586	89.7786	96.8990	100.7207	110.7657	91.6898	79.7247	111.2392	101.9145	85.9381	98.3142
a_3	−200.1014	−198.2336	−210.2945	−187.1111	−167.4654	−179.7048	−202.6287	−206.6067	−199.7036	−188.7557	−208.7630
a_4	289.1036	375.1405	318.5853	302.9995	297.3273	360.1928	350.1520	325.2051	378.4956	398.9698	341.7952
a_5	−265.4304	−222.9168	−238.7594	−274.5659	−205.1692	−297.9199	−301.6974	−269.9160	−241.8707	−250.9096	−225.3736
a_6	79.9026	91.1474	99.8885	86.3146	55.1304	69.2458	92.8226	64.1757	95.4982	79.2156	80.3134
b_0	12.2575	10.1718	30.4343	23.3592	20.1003	17.1419	11.2923	9.6965	16.8973	21.0296	15.2065
b_1	−125.2630	−140.5759	−145.0790	−150.5398	−134.8022	−120.1509	−138.4204	−145.5454	−124.7027	−117.9474	−115.4756
b_2	400.2939	505.1158	477.5352	563.3992	489.2882	471.6863	523.9821	512.4536	469.5230	485.1155	530.7250
b_3	−925.9014	−999.6598	−851.6390	−874.8194	−905.6473	−963.5568	−812.2813	−887.7445	−945.4015	−824.9164	−911.4074
b_4	1241.7436	1300.4585	1225.7009	1150.4076	1281.2225	1200.4156	1269.2198	1250.3201	1195.2240	1312.8904	1275.3236
b_5	−707.6116	−714.8203	−680.4270	−750.7814	−697.3104	−760.1877	−720.8627	−777.6309	−685.1064	−711.8785	−730.7766
b_6	177.1086	197.4633	164.1537	185.7426	155.2871	161.8064	149.8930	185.8250	123.4602	201.9203	134.9338
Eq. (21)											
a_0	1.1278	0.7955	0.8490	1.0164	0.9630	0.9295	1.0516	0.9245	0.9888	1.0989	1.1354
a_1	0.9789	0.8439	0.7985	0.8510	1.1044	1.2000	0.7999	1.2331	0.1219	1.1945	1.1182
a_2	1.3484	1.6776	1.3846	1.8330	1.8698	1.7689	1.2860	1.3067	1.9288	1.2168	1.7321
a_3	−2.3143	−2.6155	−2.4477	−2.5247	−1.9864	−1.9550	−2.7765	−1.8697	−2.5991	−2.1273	−2.2932
a_4	1.6046	2.1912	1.7298	1.9164	2.3200	2.3160	1.6645	2.3982	2.5198	2.5117	1.8912
Eq. (22)											
a_0	0.1704	0.5795	0.9418	0.1931	0.3159	0.5941	0.7740	0.8810	0.7598	0.6996	0.2748
a_1	−0.1017	−0.0466	−0.3398	−0.0315	−0.2359	−0.0914	−0.1694	−0.1151	−0.1340	−0.0485	−0.0911
c_0	0.1616	0.2553	0.1452	0.1492	0.3222	0.4515	0.2805	0.3075	0.3060	0.3693	0.4205
c_1	−0.1258	−0.1900	−0.8515	−0.0369	−0.0239	−0.0760	−0.0427	−0.0710	−0.0232	−0.0564	−0.2085
c_2	−0.0431	−0.1971	−0.0895	−0.0472	−0.1643	−0.0712	−0.0977	−0.0832	−0.0353	−0.0595	−0.0504
b_0	0.7512	0.9699	1.1848	0.6585	0.8582	1.5507	1.2532	0.9266	0.8858	0.9616	0.9090
b_1	1.5863	0.9602	0.8349	1.2209	1.3500	1.3130	1.3322	1.5338	1.6114	1.4690	1.6237
b_2	−0.9008	−0.6452	−0.2955	−0.4415	−0.3555	−0.5366	−0.7005	−0.8023	−0.5367	−0.9498	−0.5369
b_3	−1.2906	−1.1832	−0.9130	−1.6756	−1.5181	−0.6977	−2.4936	−1.9311	−2.4297	−1.2415	−1.1341
b_4	1.1196	1.5928	1.0380	1.4301	1.3295	1.6635	0.8577	1.7030	1.6049	1.6873	1.6685
Eq. (23)											
a_0	0.9237	0.9546	0.8591	1.0457	1.0078	1.1426	1.0658	1.1769	1.1013	1.0215	0.9991
a_1	−1.5944	−1.8065	−1.0305	−1.7807	−1.5123	−1.2685	−1.6932	−1.8750	−1.9345	−1.1633	−1.2911
a_2	1.4910	1.1961	1.4801	1.6313	1.7802	1.9290	1.6889	1.5471	1.9232	1.5406	1.5774
a_3	−0.5045	−0.9082	−0.5401	−0.8468	−1.2402	−0.7031	−1.2997	−1.3899	−0.6139	−1.4053	−0.9271
a_4	0.1691	0.2583	0.8386	0.1172	0.2183	0.1331	0.1459	0.1639	0.2663	0.4048	0.5017
b_0	−0.1475	−0.4908	−0.2453	−0.2381	−0.1930	−0.2464	−0.1167	−0.2775	−0.3877	0.2138	0.2800
b_1	0.3936	0.6255	0.7937	0.8723	0.9885	0.3403	0.9230	0.5377	0.5324	0.1234	0.3024
b_2	−0.0788	−0.0958	−0.4074	−0.0130	−0.0344	−0.0412	−0.0212	−0.0715	−0.0950	−0.0812	−0.1439
b_3	−0.0247	−0.0444	−0.5809	−0.0571	−0.0986	−0.0653	−0.0826	−0.0673	−0.0325	−0.0559	−0.0197
b_4	0.8583	0.8467	0.9535	0.9651	1.0002	0.9752	0.9736	1.0066	0.9032	1.1348	0.8155
Eq. (24)											
a_0	0.2460	0.4161	0.4562	0.2525	0.3958	0.3565	0.1419	0.2463	0.3942	0.3905	0.3069
a_1	0.1202	0.1873	0.1806	0.1746	0.2739	0.2780	0.1672	0.1348	0.1415	0.3984	0.3195
a_2	0.3704	0.3878	0.8206	0.9808	0.4860	0.7096	0.6277	0.7660	0.5270	0.5532	0.2534
a_3	0.7872	0.1991	0.4587	0.6378	0.3589	0.3845	0.3397	0.4229	0.8887	0.6658	0.3048
Eq. (25)											
δ	0.4359	0.4119	0.4195	0.1330	0.8724	0.0561	0.6827	0.3716	0.6354	0.8796	0.4114
c_0	0.7885	0.1887	0.9206	0.6706	0.9045	0.9032	0.1506	0.4059	0.7984	0.6710	0.5605
c_1	−0.5214	−0.1829	−0.1358	−0.2606	−0.5895	−0.6440	−0.5259	−0.3548	−0.3120	−0.6672	−0.6436
c_2	1.5579	1.7272	1.5768	1.5816	0.8496	2.1506	2.1369	1.5607	20.1661	1.3143	0.8827

$$MSE = \frac{\sum_{i=1}^{N}\left(\rho_{Calc.}(i) - \rho_{Exp.}(i)\right)^2}{N} \tag{39}$$

$$STD = \sum_{i=0}^{N}\sqrt{\frac{\left(\rho_{Calc.}(i) - \bar{\rho}_{Exp.}(i)\right)^2}{N}} \tag{40}$$

For example, Fig. 4 indicates the total results of the correlation factor based on Eq. (20) and C$_4$mim-family with applying test data subcategories. The solid 45° line shows the details of fitting between the experimental data and the related ones, whereas circles point show the comparison between the obtained results based on Eq. (20) and the experimental density data. The R^2 value is 0.9856. Indeed, closeness of the circle

Table 6 The values of evaluation criteria.

|	BuPy	C$_2$mim	C$_3$mim	C$_4$mim	C$_6$mim	C$_8$mim	Hmim	Mmim	Moim	OcPy	Omim
Eq. (20)											
R^2	0.9843	0.9826	0.9810	0.9672	0.9965	0.9610	0.9850	0.9660	0.9882	0.9817	0.9779
RMSE	0.0151	0.0268	0.0658	0.0235	0.0425	0.0630	0.0409	0.0604	0.0563	0.0634	0.0261
Mse $\times 10^3$	0.1459	0.4930	0.1256	0.5311	0.3114	0.6735	0.2278	0.1295	0.5176	0.4596	0.3616
AAPD	0.6203	0.1036	0.5026	0.2572	0.3013	0.3208	0.1818	0.0895	0.2943	0.2166	0.2724
STD	1.2825	0.8968	0.7412	0.9432	0.6912	1.2285	0.8310	0.6492	0.5619	0.9588	1.0348
Eq. (21)											
R^2	0.9694	0.9877	0.9866	0.9665	0.9765	0.9671	0.9622	0.9891	0.9820	0.9889	0.9796
RMSE	0.0490	0.0417	0.0980	0.0186	0.0332	0.0246	0.0678	0.0568	0.0542	0.0178	0.0203
Mse $\times 10^3$	0.5543	0.2363	0.6750	0.6876	0.3615	0.1061	0.6381	0.1885	0.2560	0.3759	0.2241
AAPD	0.2200	0.3742	0.7296	0.8094	0.2403	0.1911	0.2633	0.2744	0.5545	0.1070	0.4451
STD	0.6077	1.0013	1.3647	0.7242	0.8031	0.7237	1.2732	0.9935	0.9702	0.6824	1.2029
Eq. (22)											
R^2	0.9648	0.9874	0.9902	0.9611	0.9814	0.9829	0.9879	0.9798	0.9894	0.9969	0.9874
RMSE	0.0602	0.0236	0.0820	0.0465	0.0329	0.0677	0.0191	0.0102	0.0605	0.0515	0.0772
Mse $\times 10^3$	0.5845	0.1933	0.4885	0.6527	0.2146	0.5924	0.6365	0.1818	0.2674	0.6023	0.2503
AAPD	0.6905	0.1205	0.3155	0.7333	0.2660	0.3034	0.8785	0.2799	0.3015	0.2622	0.1240
STD	0.8942	0.5669	0.4012	0.6171	1.2187	0.6396	1.2972	1.2513	0.5196	0.7305	0.8006
Eq. (23)											
R^2	0.9780	0.9671	0.9856	0.9683	0.9975	0.9744	0.9727	0.9822	0.9631	0.9927	0.9839
RMSE	0.0243	0.0233	0.0642	0.0660	0.0592	0.0306	0.0114	0.0298	0.0456	0.0598	0.0600
Mse $\times 10^3$	0.2669	0.1757	0.7953	0.6583	0.5247	0.2842	0.6188	0.4152	0.5709	0.3258	0.1862
AAPD	0.0726	0.6398	0.2103	0.2083	0.2473	0.8620	0.1735	0.0448	0.5440	0.7945	0.9860
STD	0.6415	0.8807	0.6718	1.0162	0.7894	0.9218	0.6626	0.8150	0.7477	0.8000	0.8267
Eq. (24)											
R^2	0.9834	0.9629	0.9600	0.9725	0.9838	0.9812	0.9793	0.9633	0.9940	0.9865	0.9909
RMSE	0.0168	0.0574	0.0419	0.0217	0.0496	0.0196	0.0622	0.0135	0.0286	0.0589	0.0641
Mse $\times 10^3$	0.3712	0.2964	0.8294	0.3186	0.2629	0.1378	0.2661	0.3379	0.4493	0.5525	0.6964
AAPD	0.1296	0.1990	0.7658	0.3636	0.4531	0.8402	0.2328	0.2751	0.1893	0.5120	0.0473
STD	0.6227	0.9080	1.0767	1.0769	0.7726	0.8680	0.6457	1.1202	0.5200	0.7332	0.8881
Eq. (25)											
R^2	0.9874	0.9953	0.9705	0.9864	0.9806	0.9634	0.9818	0.9694	0.9868	0.9850	0.9878
RMSE	0.0529	0.0387	0.0952	0.0571	0.0569	0.0529	0.0282	0.0508	0.0474	0.0142	0.0350
Mse $\times 10^3$	0.6510	0.2341	0.8651	0.6813	0.3055	0.3780	0.1360	0.4671	0.2850	0.5357	0.2802
AAPD	0.0558	0.6734	0.5588	0.4156	0.9137	0.6346	0.0422	0.2637	0.2711	0.0939	0.6510
STD	1.0151	0.6302	1.0973	0.5869	0.6230	1.1140	0.6719	0.9082	0.8108	1.0359	0.6241
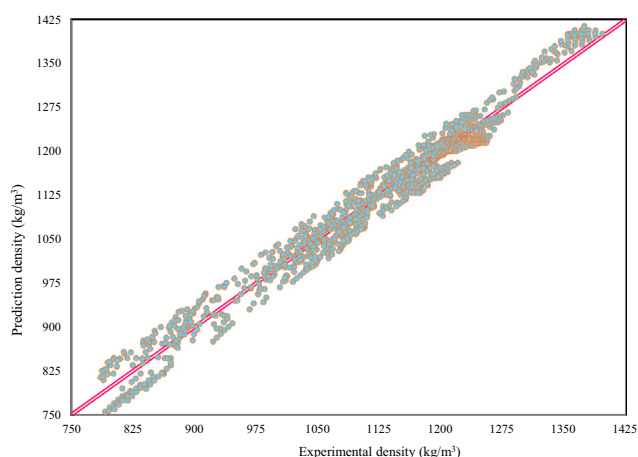
Fig. 4 Predicted versus experimental IL density mixtures for test datasets. The reported results are related to Eq. (23) and C$_4$mim-family.

points to the solid line in Fig. 4 demonstrates the presented modification technique has acceptable ability to predict IL-mixture density.

The six semi-empirical equations gave different results and any cation-family presented various results to predict the density of IL-mixture system at all temperatures. For example, Fig. 5 indicates the density behavior of OmimBF$_4$ + ethanol (x_{IL} = 0.247 and x_{IL} = 0.839) and C$_4$mimClO$_4$ + ethanol (x_{IL} = 0.709 and x_{IL} = 0.900) based on semi-empirical equations (using test data). According to Fig. 5, the semi-empirical equations could predict the mixture density with acceptable accuracy. All semi-empirical equations have similar behavior and they could predict the mixture density with acceptable accuracy.

All semi-empirical equations, except Eq. (24), only were used to predict pure IL density up to now. For first time, we have examined the capability of these equations to predict the density of IL-mixture system at various mole fractions and temperatures. Subsequently, mixing rules had significant
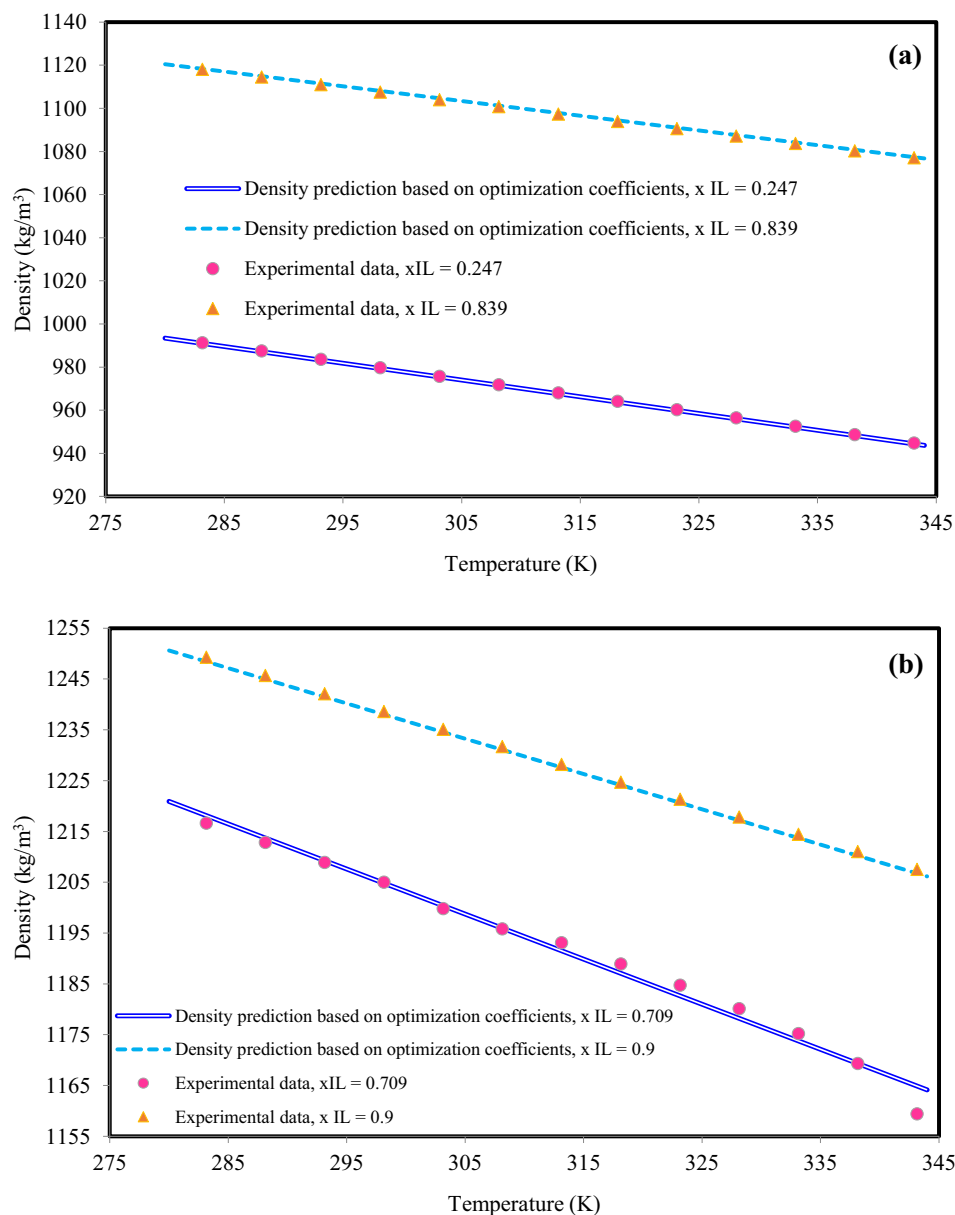
Fig. 5   The density behavior of (a) OmimBF$_4$ + ethanol, x_{IL} = 0.247 and x_{IL} = 0.839 (b) C$_4$mimClO$_4$ + ethanol, x_{IL} = 0.709 and x_{IL} = 0.900. The obtained results based on Eq. (20) with optimized coefficients. The experimental data are from Mokhtarani et al. (Mokhtarani et al., 2008).

role in this development and they show the effect of component mole fraction. According to Table 3 various mixing rules, at least three mixing rules for each property, was investigated. The mixing rule of all thermodynamic properties except acentric factor and critical temperature, was linear. The experimental data density mixture are function of mole fraction and temperature and all semi-empirical equations are function of reduced temperature (T_r), therefore, critical temperature mixing rule have remarkable influence on accuracy of obtained results based on semi-empirical equations. Several critical temperature mixing rules have been investigated but non-linear ones indicated better results. This mixing rule is function of second power of mole fraction and also second order of radical of both IL and solvent critical temperature ($\sqrt{T_{ci}T_{cj}}$).

To more investigation of accuracy of obtained confidents, the density behavior of IL binary systems that was unused in the optimization coefficients procedure was model. For instance, Fig. 6 indicates the results of BuPyBF$_4$ + water, x_{IL} = 0.144 and x_{IL} = 0.737 and OcPyBF$_4$ + water, x_{IL} = 0.242 and x_{IL} = 0.816 binary systems. The obtained results indicated the all semi-empirical equation can predict the behavior of density of IL-mixture with satisfactory accuracy and it demonstrates the accuracy of presented models. Furthermore, the values of AAPD of all binary systems are provided in Table 7. According to Table 7, the AAPD of Eqs. (20) - (25), SRK EoS and PT EoS are 0.7312, 0.7666, 0.7631, 0.7583, 0.7750, 0.7560, 22.0470, 18.9372, respectively. Indeed, Eqs. (21) - (23) have almost the similar functionality of temper-
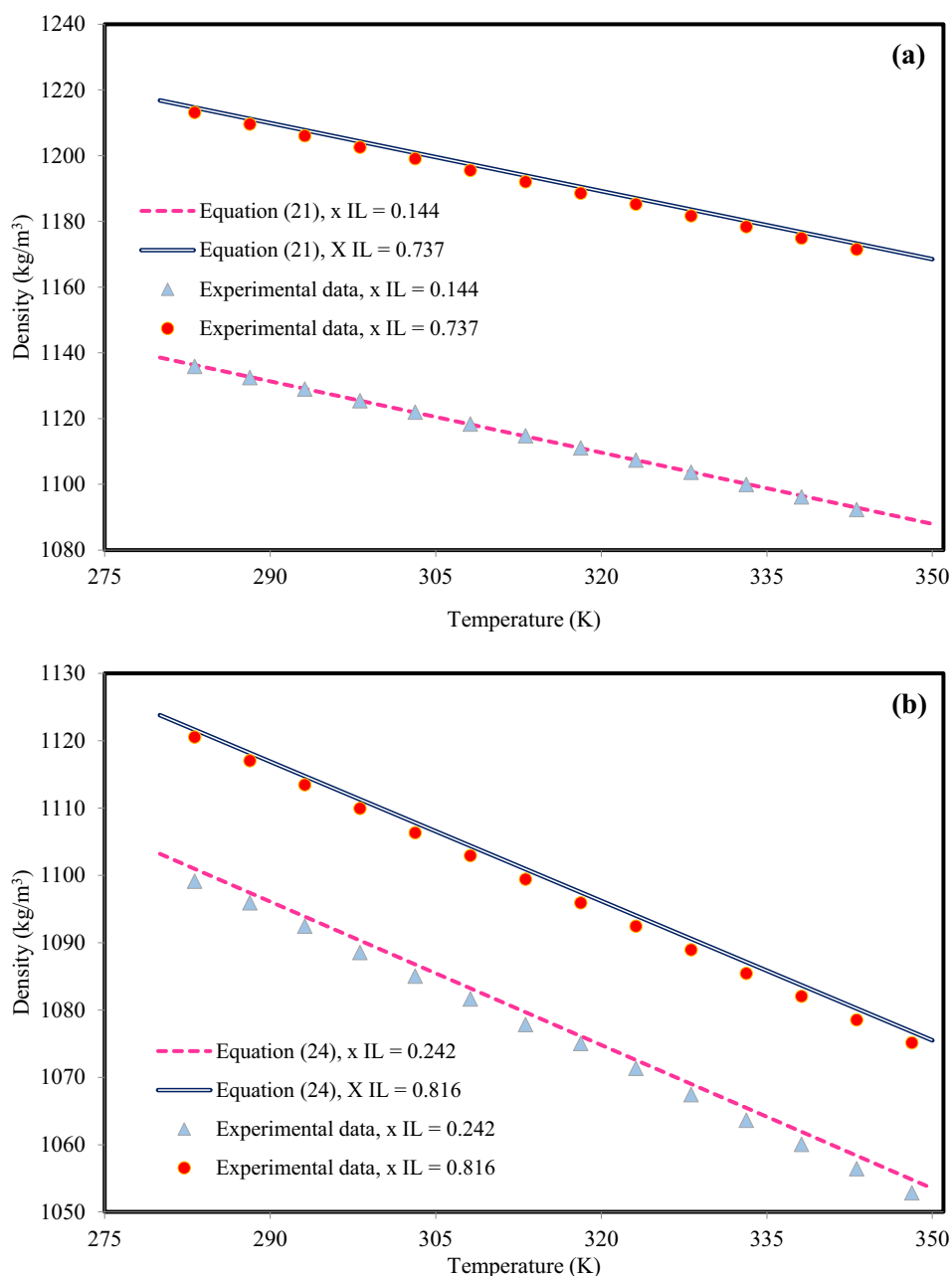
Fig. 6 The density behavior of (a) BuPyBF$_4$ + water, x$_{IL}$ = 0.144 and x$_{IL}$ = 0.737 and (b) OcPyBF$_4$ + water, x$_{IL}$ = 0.242 and x$_{IL}$ = 0.816. The experimental data are from Mokhtarani et al. (Mokhtarani et al., 2009).

ature and they need the similar input, subsequently, the AAPD of them is almost similar. Also, the results of NM equation are considerable. This equation requires critical temperature, molecular weight and critical volume as input but the temperature functionality of NM equation is contained two different non-linear expressions.

In the case of density mixtures, as mentioned, influence of mixing rule to extend the critical properties and molecular weight is significant and it affect the accuracy of semi-empirical equation. According to Table 3, different mixing rules were applied to generalize the pure thermodynamics properties to binary mixtures. After investigation the accuracy and comparison the AAPD values of obtained results, the final mixing rules for each thermodynamics properties were selected. For example, the

obtained results of C$_2$mimBF$_4$ + acetone binary system at x$_{IL}$ = 0.5772 and x$_{IL}$ = 0.8304 based on equation (25) and C$_2$mimBF$_4$ + dimethylsulphoxide binary system at x$_{IL}$ = 0.3417 and x$_{IL}$ = 0.6717 based on equation (23) are presented in Fig. 7. The optimization process was performed based on both final and linear mixing rules ($Q = \sum_i x_i Q_i : Q = M_w$, T_c, V_c, P_c, ω). According to Fig. 7, the selection of mixing rules had considerable effect on the optimized coefficient and furthermore, prediction of density of IL-mixture.

4. Conclusion

In the present communication, six semi-empirical equations with various mixing rules was employed to calculate the den-

Table 7 The AAPD values of Eqs. (20)–(25) and CEoSs.

System number*	Eq. (20)	Eq. (21)	Eq. (22)	Eq. (23)	Eq. (24)	Eq. (25)	SRK EoS	PT EoS
1	0.2366	0.9938	0.6236	0.2660	0.5182	0.1118	20.6262	18.3660
2	0.3138	0.9736	0.4391	0.6749	0.7861	0.9652	22.2795	25.7948
3	0.4822	0.4050	0.5199	0.8488	0.7260	0.3481	17.8561	31.2398
4	0.9775	0.3402	0.3065	0.7040	0.3442	0.8307	19.7477	16.4109
5	0.6457	0.5299	0.1762	0.6311	0.7489	0.3351	24.2136	18.8411
6	0.0599	0.7519	0.4793	0.5294	0.6676	0.2002	17.4252	29.3787
7	0.4855	0.3745	0.2577	0.2571	0.1959	0.3253	19.9113	14.9408
8	0.0024	0.8064	0.5500	0.5801	0.2602	0.7941	22.6095	30.5583
9	0.1135	1.0045	0.4547	0.3476	0.3795	0.8473	28.3839	20.2513
10	0.0138	0.5264	0.8608	0.7882	0.6452	0.3883	17.4518	18.5096
11	0.1767	0.2741	0.4487	0.8825	0.8156	0.6651	24.2974	19.3817
12	0.3506	0.3614	0.5615	0.1624	0.4078	0.4751	20.3464	13.5489
13	0.1209	0.5865	0.1637	0.8849	0.8533	0.8700	30.0776	21.9492
14	0.0255	0.6330	0.4872	0.7121	0.3213	0.7359	18.3771	14.7050
15	1.1136	0.4185	0.9857	0.5823	0.6095	0.8825	22.2321	23.5823
16	1.2179	0.4185	0.7488	0.4786	0.7445	1.1079	15.9280	11.2609
17	0.5172	0.8909	0.8568	0.5696	0.6746	0.7641	14.2380	10.9519
18	0.7567	0.7174	0.7288	0.8311	0.8608	0.4860	17.4102	20.8407
19	1.1845	0.4581	1.3931	0.6394	1.1597	0.6883	25.1026	23.3282
20	0.8233	1.1454	0.7946	0.7233	0.5799	0.7766	16.0869	14.5742
21	0.9013	1.0476	0.3938	1.0127	0.9457	1.0858	17.1235	18.5200
22	0.9249	0.9706	0.4059	0.6363	1.4645	0.8279	20.4922	18.4954
23	1.0355	0.8541	1.0774	0.3261	0.7345	0.9145	21.3880	19.2354
24	0.7399	0.5475	0.8528	1.1006	1.1143	1.1042	13.2281	15.3350
25	0.4353	0.6610	0.6409	0.6654	0.4502	0.4738	25.0577	21.5457
26	0.6793	0.7609	1.1913	0.9286	0.8049	1.3186	18.1603	14.2094
27	0.9769	1.0715	0.9096	1.1884	1.0869	0.5985	19.4429	16.5605
28	0.7649	1.1982	1.1568	0.8768	0.6276	0.5799	23.2291	18.4369
29	0.8012	0.7374	0.8162	0.9983	1.0290	1.0849	17.5259	14.2769
30	1.0510	0.8341	0.4441	1.0620	0.7719	1.1473	15.2965	13.3316
31	0.8245	0.6287	0.9059	0.9214	0.9887	0.6440	20.0022	16.4984
32	0.5583	0.8584	0.8950	1.3014	1.1800	0.9410	23.1882	19.5751
33	0.9300	1.1585	1.0751	0.6562	0.4595	0.7722	16.0683	15.3228
34	0.7717	0.7922	0.8343	0.8596	1.1295	0.9228	22.1401	20.1552
35	0.8754	0.7628	0.6590	1.1077	0.7437	0.6417	21.2102	18.2696
36	0.7837	0.3913	1.1158	0.5664	0.8120	0.4831	25.2277	23.5010
37	0.3936	1.0511	0.6216	0.9803	0.7890	1.2878	22.3686	19.6221
38	0.9286	0.5020	0.7248	0.7647	0.9881	0.5595	20.2726	17.3448
39	0.7720	0.7740	0.5062	1.0887	1.1570	0.8122	24.0508	23.4803
40	0.9569	0.9026	0.7202	0.5310	0.4262	1.2882	25.2024	20.3102
41	1.0547	1.0610	0.9624	0.6344	0.6095	0.7403	19.5668	16.2232
42	0.7944	0.8800	0.7353	0.8147	0.8221	1.1154	15.0228	13.5625
43	1.3939	0.9507	0.5585	1.0797	0.4545	1.3330	20.2113	22.2219
44	0.7020	0.7874	0.9803	0.7192	1.3622	0.8104	17.1145	18.4901
45	0.9286	1.1702	0.6608	1.1069	0.6355	0.6103	23.4376	17.1839
46	0.8677	0.9151	0.8137	0.5581	1.1561	0.7747	16.2416	11.3694
47	1.0205	0.4208	0.7411	0.9023	0.5926	0.5682	18.5587	16.4248
48	0.6093	0.8715	0.8273	0.7207	0.6800	0.6479	22.1217	14.3894
49	1.1242	0.5098	0.5184	1.0568	0.9178	0.9191	20.4540	15.1821
50	0.9328	0.7951	0.7125	0.8855	1.0723	0.7718	26.1576	19.5411
51	1.0071	0.6699	0.9141	1.0862	0.5984	0.6173	17.4104	20.3195
52	1.0873	0.5733	0.7026	0.6897	0.8417	0.7947	20.4437	25.4147
53	0.9315	0.9009	0.4173	0.8277	0.9166	0.8500	26.1834	22.4174
54	0.8387	1.1847	1.1503	0.6041	0.6460	0.6555	27.2895	20.3707
55	0.6351	0.3769	0.8066	0.2743	1.0362	1.3064	19.4910	16.1931
56	1.1824	0.5897	1.2777	0.4010	0.4390	0.7860	30.2903	25.2651
57	0.9700	0.9605	1.4981	0.7703	0.5992	1.0047	20.5929	14.6114
58	0.7653	1.0829	0.7731	1.0306	0.9872	1.2551	24.4616	19.4590
59	0.6842	0.5678	0.8767	0.7822	1.1243	0.5189	22.3143	17.2093
60	0.9165	1.2557	0.7068	0.9975	0.6618	0.8639	28.2994	20.3600
61	1.0381	0.9686	0.5094	0.6778	1.0406	0.8255	25.4474	16.5362
62	0.9058	1.0349	0.7562	0.3886	0.6784	0.7343	17.1212	22.2459
63	0.7250	0.7988	0.9334	0.7909	0.7682	1.1759	20.3667	16.1150

Table 7 (*continued*)

System number*	Eq. (20)	Eq. (21)	Eq. (22)	Eq. (23)	Eq. (24)	Eq. (25)	SRK EoS	PT EoS
64	0.8682	1.0271	0.7306	1.1561	0.8568	0.6108	31.2142	25.2189
65	0.4962	0.4970	0.5676	0.7679	0.5670	0.8960	19.3296	12.3942
66	1.0135	0.9702	0.6312	1.1071	0.9584	0.5956	22.2232	20.4761
67	0.6528	0.6173	1.0526	0.4040	1.1928	1.3312	32.3213	26.5113
68	1.0590	1.0087	0.9463	1.3112	0.8234	0.9441	23.2044	19.3744
69	0.9628	0.7772	1.2073	0.4152	0.6455	1.1672	25.4590	15.4579
70	0.6561	0.7240	0.8028	0.5473	1.0702	0.7092	26.3738	22.3680
71	0.9642	0.4912	0.7451	1.0189	0.6651	0.5748	20.1293	24.1283
72	0.8688	1.1057	0.9951	0.8658	0.9186	1.0616	19.3760	13.5043
73	1.1162	0.7521	1.1260	1.0728	0.5636	0.9677	26.2362	17.3098
74	0.9265	0.7323	1.0939	0.8414	1.0548	0.3449	29.4522	25.1483
75	0.8010	1.0950	0.9583	0.5727	0.9696	1.0753	26.3080	20.2611
76	0.5967	0.4691	0.8234	1.1601	0.7618	0.5173	22.1527	18.1489
77	0.9746	1.1053	0.9506	0.6131	0.4281	1.1279	18.3662	11.2910
78	1.1670	0.8141	0.6111	1.0475	0.6152	0.9081	20.1981	14.4174
79	0.7856	1.1656	0.7128	0.6545	1.1571	0.9243	27.0376	19.2677
80	0.6580	0.8298	1.0294	0.7007	0.6109	1.1576	16.4658	10.3470
81	1.0063	0.9674	0.9832	0.8751	1.0015	0.9081	25.2930	19.5448
82	0.5515	1.0584	0.7457	0.2872	0.6918	1.0400	23.1865	20.4934
83	1.0324	1.0120	0.6887	0.7416	1.1276	0.8326	22.0761	26.1072
84	0.4616	0.2522	1.1657	0.5994	0.6575	1.1419	19.5836	23.2855
85	1.0995	0.7428	0.8728	1.0030	0.3680	0.6658	17.1113	12.5065
86	0.5938	1.0764	0.9620	1.0255	1.0601	0.8125	20.2285	13.3925
87	1.1246	1.2448	1.1656	0.8523	0.5949	0.4132	23.5275	17.4630
88	0.9295	0.8751	0.5092	1.1403	0.7628	0.3559	16.3271	22.1459
89	0.8602	0.3406	1.0966	0.8856	0.9862	1.0417	26.4708	18.3663
90	1.1492	0.4746	0.8574	1.1516	1.1790	0.4501	17.2814	23.1822
91	0.7055	1.1907	0.5293	0.4263	0.8536	0.9265	26.3938	20.4300
92	1.0513	0.6945	1.0913	0.3350	0.9183	0.4481	20.0959	12.3902
93	0.5322	1.0568	0.8131	0.9647	0.6648	1.0756	18.2427	25.4996
94	0.5131	0.4318	1.2280	0.6211	0.3784	0.7032	20.3507	16.3106
95	0.4457	0.6764	0.9205	1.1251	0.5122	0.3348	27.4560	19.0258
96	1.1939	0.6925	0.5570	0.7361	0.6118	0.6541	30.3385	24.3835
97	0.9260	1.0649	0.8042	0.5577	1.0655	0.5390	20.5021	26.6911
98	0.5716	0.4146	0.7446	0.9852	0.7023	0.4653	23.2957	19.2800
99	1.1555	0.9556	0.9868	1.1887	0.3375	0.8093	24.4195	20.4356
100	0.9246	0.7489	0.8192	0.6692	1.0280	1.1993	19.1761	15.3610
101	0.7495	1.0863	1.2728	1.1763	0.7377	0.7280	25.2438	19.5895
102	0.8335	0.3809	0.9006	0.5686	1.0282	0.5233	20.3450	15.2570
103	1.0173	1.0885	0.7667	0.7837	0.7383	0.3304	26.2945	19.3476
104	0.9434	1.1998	1.0156	1.0830	0.8712	0.9216	23.3907	20.4538
105	1.0471	0.1241	0.0436	0.1824	0.3021	1.1070	19.6531	14.7969
106	0.4073	0.6530	0.0282	0.7868	0.9569	0.8697	22.9742	17.6829
107	0.2090	0.6049	0.9676	0.3350	0.5228	0.2784	26.1503	20.5382
108	0.7435	0.9946	0.5816	0.2269	0.8929	0.3780	23.6544	18.8334
109	0.2463	0.7650	0.6785	0.6209	0.4821	0.7939	17.3563	13.3656
110	0.4968	0.6024	0.2164	0.1852	0.6014	0.5938	24.5270	20.9553
111	0.8723	0.9480	0.8896	1.0091	0.7773	0.9340	16.4367	11.7906
112	0.7836	0.5759	0.4184	0.6427	0.7976	0.4819	27.6427	23.4184
113	0.2562	0.8570	0.1923	0.7249	0.3573	0.1481	21.3660	17.5832
114	0.3278	0.1728	0.4784	0.2393	1.0286	0.8061	20.1862	22.8198
115	0.2654	0.5318	1.0878	0.6776	0.8433	0.2049	30.2989	24.8862
116	0.1344	0.1149	0.7160	0.3176	0.1619	0.4388	28.2236	23.3719
117	0.4082	1.1505	0.5350	1.1786	1.4210	0.6877	23.4463	17.2598
118	1.0533	0.4865	0.6443	0.7387	0.3543	0.8803	21.2917	15.3503
119	0.7894	0.9125	0.9461	0.9538	0.7117	1.0629	18.5784	23.5890
120	0.1277	0.8769	0.3354	0.7117	0.9756	0.7431	26.8781	20.6559
121	0.3077	0.7126	0.4122	0.4314	0.8272	0.9128	24.3818	19.3874
122	0.4527	0.4187	0.6633	1.0881	1.1240	0.3716	25.7595	18.2520
123	0.7520	0.2798	0.8228	0.3768	1.0647	0.3627	18.2413	13.3981
124	0.6198	0.9099	1.1055	0.9867	0.6933	0.5579	23.3374	19.1641
125	0.4934	0.3213	0.8309	0.4075	0.6011	0.5841	30.3836	24.2541
126	0.8331	0.8488	0.5991	0.9630	1.1515	0.3296	19.1895	14.7146

Table 7 (*continued*)

System number*	Eq. (20)	Eq. (21)	Eq. (22)	Eq. (23)	Eq. (24)	Eq. (25)	SRK EoS	PT EoS
127	0.1512	1.1110	1.0555	1.1976	0.4223	0.9994	27.5462	23.5352
128	1.0881	0.6283	0.3094	0.5494	0.9735	0.1587	18.6711	15.2730
129	0.0558	0.9169	0.8610	0.7337	0.4125	0.5869	20.4749	16.4600
130	0.3635	0.7954	0.6822	0.8151	0.9161	1.0103	23.1087	20.3927
Average AAPD	0.7312	0.7666	0.7631	0.7583	0.7750	0.7560	22.0470	18.9372

* System number according to Table 2.
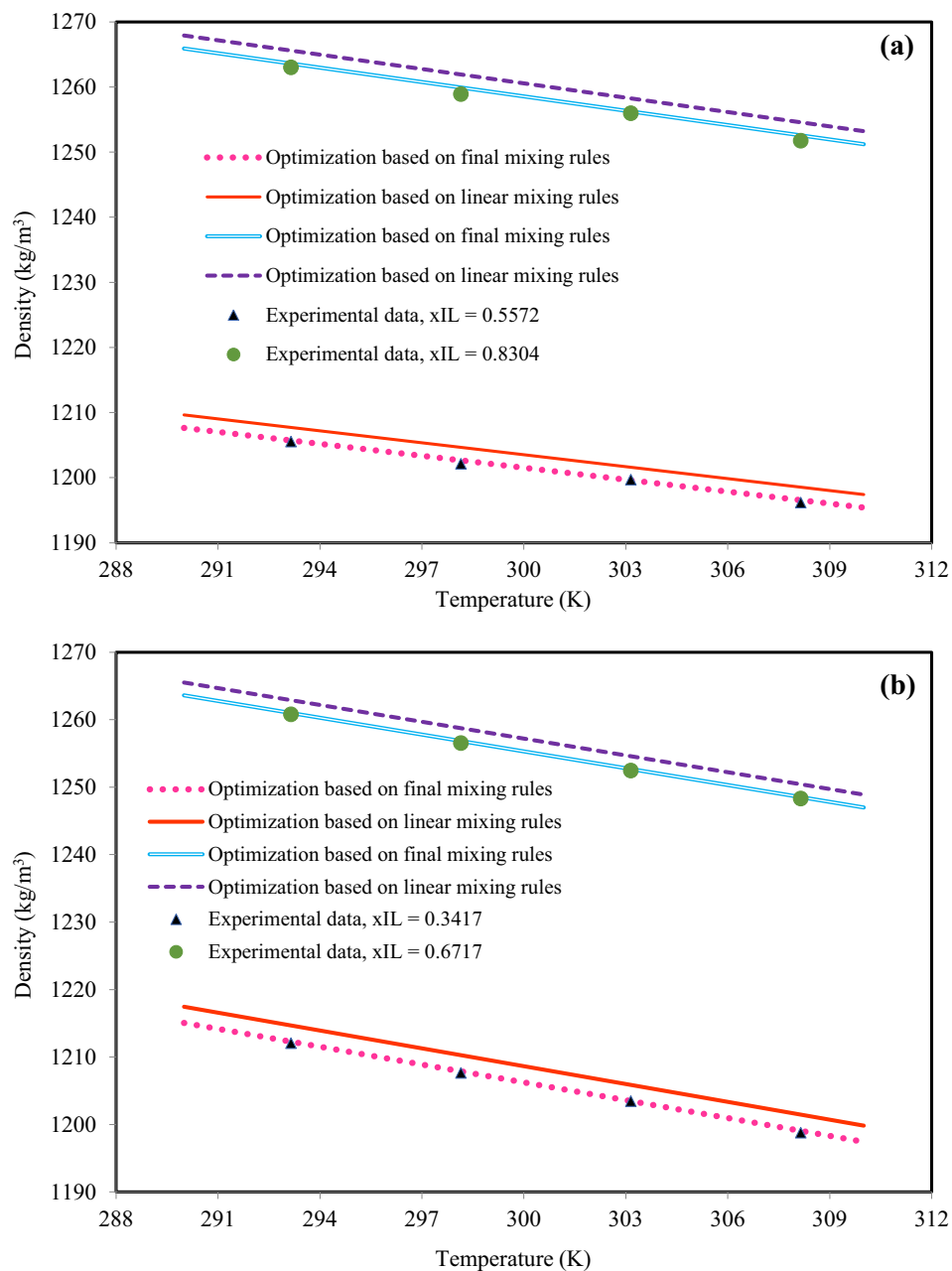
Fig. 7 The density behavior of (a) C_2mimBF_4 + acetone, $x_{IL} = 0.5772$ and $x_{IL} = 0.8304$ based on equation (25) and (b) C_2mimBF_4 + dimethylsulphoxide, $x_{IL} = 0.3417$ and $x_{IL} = 0.6717$ based on equation (23). The experimental data are from Bhagour et al. (Bhagour et al., 2013).

Table A1   Generalized models for liquid density considered in this study Valderrama and Zarricuetac, 2009, Hosseini et al., 2013.

Model	Parameters
$\ln \frac{M_w P_c}{R\rho T} = \ln V^0 + \omega \ln V^1 \ln V^0 = a_0 + a_1 T_r + a_2 T_r^2 + a_3 T_r^3 + a_4 T_r^4 + a_5 T_r^5 + a_6 T_r^6 \ln V^1$ $= b_0 + b_1 T_r + b_2 T_r^2 + b_3 T_r^3 + b_4 T_r^4 + b_5 T_r^5 + b_6 T_r^6$	ω, M_w, T_c, P_c
$\rho = \frac{M_w}{V_c}\left(a_0 + a_1 \tau^{\frac{1}{3}} + a_2 \tau^{\frac{2}{3}} + a_3 \tau + a_4 \tau^{\frac{4}{3}}\right)\tau = 1 - \frac{T_r}{\left[1+(0.48+1.574\omega-0.176\omega^2)\left(1-\sqrt{T_r}\right)\right]^2}$	ω, M_w, T_c, V_c
$\rho = \frac{P_c M_w}{RT_c V_1 (1-\omega V_2)(a_0 + a_1\omega)} 0.2 < T_r < 0.8 : V_1 = b_0 + b_1 T_r + b_2 T_r^2 + b_3 T_r^3 + b_4 T_r^4 0.8 < T_r < 1 :$ $V_1 = b_0 + b_1 \sqrt{1-T_r} \log (1-T_r) + b_2 (1-T_r) + + b_3 (1-T_r)^2 , V_2 = c_0 + c_1 T_r + c_2 T_r^2$	ω, M_w, T_c, P_c
$\rho = \frac{M_w}{V_c\left[V^0 + \left(1 - \frac{\omega(b_0 + b_1 T_r + b_2 T_r^2 + b_3 T_r^2)}{T_r + b_4}\right)\right]} V^0 = a_0 + a_1(1-T_r)^{\frac{1}{3}} + a_2(1-T_r)^{\frac{2}{3}} + a_3(1-T_r) + a_4(1-T_r)^{\frac{4}{3}}$	ω, M_w, T_c, V_c
$\rho = \left(\sum_i \frac{P_{ci} M_{wi}}{RT_{ci} x_i}\right)\left(a_0 + a_1\omega + a_2\omega^2 + a_3\omega^4\right)^{-\left(1+(1-T_r)^{\frac{2}{7}}\right)}$	ω, M_w, T_c, P_c
$\rho = \frac{M_w}{V_c}\rho_0\left[1 + \delta(f(T_r)-1)^{\frac{1}{3}}\right]\rho_0 = 1 + 1.1688\left(1 - \frac{T_r}{f(T_r)}\right)^{\frac{1}{3}} + 1.8177\left(1 - \frac{T_r}{f(T_r)}\right)^{\frac{2}{3}}$ $-2.65811.1688\left(1 - \frac{T_r}{f(T_r)}\right) + 2.1613\left(1 - \frac{T_r}{f(T_r)}\right)^{\frac{4}{3}}$	M_w, T_c, V_c
$\rho = \frac{M_w}{V_c}\left[a_0 + a_1(1-T_r) + (a_2 + a_3\omega)(1-T_r)^{\frac{1}{3}}\right]$	ω, M_w, T_c, V_c
$\rho = \frac{M_w(Z_c)^{-(1-T_r)^{0.29}}}{V_c}$	Z_c, M_w, T_c, V_c
$\rho = \frac{M_w}{V_c}\left[1 + \sum_{i=1}^{4} k_i(1-T_r)^{i/3}\right]$	M_w, T_c, V_c
$\rho = \frac{M_w}{V_c}(0.29056 - 0.08775\omega)^{-(1-T_r)^{0.29}}$	ω, M_w, T_c, V_c

sity of 130 different IL-mixture binary systems. The considered systems covered 51 ILs (11 cation-family) and 41 solvents. The used semi-empirical equations had unknown coefficients and to present comprehensive IL-mixture density, the unknown coefficients was obtained using laplacian whale optimization algorithm for each cation-family, separately. Regarding the presentation in the field of cost function, the obtained results were highly accurate. To obtained of unknown coefficients, 70% of experimental data of each cation-family according to SSMD method were used and the remaining experimental data were applied to investigate the accuracy of presented models. The obtained results based on both test and train data were acceptable and the performed modification on semi-empirical equations to generalize binary mixture was successful. Beside the semi-empirical equations, capability of SRK EoS and PT EoS cubic equations state to was investigated predict IL-mixture density; however, the obtained results based on both CEoSs had significant deviation from experimental data therefore, that using binary interaction parameter could not decrease deviation, remarkably.

Declaration of Competing Interest

The authors declare that they have no known competing financial interests or personal relationships that could have appeared to influence the work reported in this paper.

Appendix A. The list of all semi-empirical equations that are used in this study, are given in Table A.1.

References

Nishan, U., Niaz, A., Muhammad, N., Asad, M., Shah, A.A., Khan, N., Khan, M., Shujah, S., Rahim, A., 2021. Arab. J. Chem. 14, 103164.

Agafonov, A.V., Kudryakova, N.O., Ramenskaya, L.M., Grishina, E.P., 2020. Arab. J. Chem. 13, 9090.

Omar, I.M.A., Al-Fakih, A.M., Aziz, M., Emran, K.M., 2021. Arab. J. Chem. 14, 102909.

Lian, C., Jian, D., Liu, H., Wu, J., 2016. J. Phys. Chem. C. 120, 8704.

Bagheri, H., Karimi, N., Dan, S., Notej, B., Ghader, S., 2021. J. Mol. Liq. 336, 116581.

Evangelista, N.S., do Carmo, F.R., de Santiago-Aguiar, R.S., de SaníAna, H.B., 2014. Ind. Eng. Chem. Res. 53, 9506.

Xu, X., Peng, C., Liu, H., Hu, Y., 2009. Ind. Eng. Chem. Res. 48, 11189.

Mohammadzadeh, M., Bagheri, H., Ghader, S., 2020. Arab. J. Chem. 13, 5821.

Mesquita, F.M.R., Coelho, L.L., Pinheiro, R.S., Ribeiro, C.A.R.C., Feitosa, F.X., de SaníAna, H.B., de Santiago-Aguiar, R.S., 2019. J. Chem. Eng. Data. 64, 3316.

Bagheri, H., Mohebbi, A., 2017. Korean J. Chem. Eng. 34, 2686.

Tao, H., Lian, C., Liu, H., 2020. Green Energy Environ. 5, 303.

Bagheri, H., Ghader, S., Hatami, N., 2019. Chem. Chem. Technol. 13, 1.

Paiva, C.L., Pinheiro, R.S., Feitosa, F.X., de SaníAna, H.B., 2019. J. Chem. Eng. Data. 64, 594.

Bagheri, H., Ghader, S., 2017. J. Mol. Liq. 236, 172.

Lian, C., Liu, K., Aken, K.L.V., Gogotsi, Y., Wesolowski, D.J., Liu, H.L., Jiang, D.E., Wu, J.Z., 2016. ACS Energy Lett. 1, 21.

Abumandour, E.S., Mutelet, F., Alonso, D., 2020. Appl. Therm. Eng. 181, 115943.

Yang, J., Lian, C., Liu, H., 2020. Chem. Eng. Sci. 227, 115927.

Bagheri, H., Hashemipour, H., Ghalandari, V., Ghader, S., 2021. Particuology. 57, 201.

Lampreia, I.M., Dias, F.A., Mendonça, Â.F., 2003. Phys. Chem. Chem. Phys. 5, 4869.

Valderrama, J.O., Zarricuetac, K., 2009. Fluid Phase Equilibr. 275, 145.

Geppert-Rybczyńska, M., Heintz, A., Lehmann, J.K., Golus, A., 2010. J. Chem. Eng. Data. 55, 4114.

Bahadur, I., Deenadayalu, N., 2011. J. Solution Chem. 40, 1528.

Matkowska, D., Hofman, T., 2013. J. Solution Chem. 42, 979.

Bahadur, I., Deenadayalu, N., Naidoo, P., Ramjugernath, D., 2013. J. Chem. Thermodyn. 57, 203.

Govinda, V., Reddy, P.M., Bahadur, I., Attri, P., Venkatesu, P., Venkateswarlu, P., 2013. Thermochim. Acta. 556, 75.

Govinda, V., Attri, P., Venkatesu, P., Venkateswarlu, P., 2013. J. Phys. Chem. B. 117, 12535.

Singh, S., Bahadur, I., Redhi, G.G., Ramjugernath, D., Ebenso, E.E., 2014. J. Mol. Liq. 200, 160.

Huang, Y., Zhang, X., Zhao, Y., Zeng, S., Dong, H., Zhang, S., 2015. Phys. Chem. Phys. 17, 26918.

Hosseini, S.M., Papari, M.M., Fadaei-Nobandegani, F., Moghadasi, J., 2013. J. Solution Chem. 42, 1854.

Abareshi, M., Goharshadi, E.K., Zebarjad, S.M., 2009. J. Mol. Liq. 149, 66.

Wang, J., Li, Z., Li, C., Wang, Z., 2010. Ind. Eng. Chem. Res. 49, 4420.

Li, J., He, C., Peng, C., Liu, H., Hu, Y., Paricaud, P., 2011. Ind. Eng. Chem. Res. 50, 7027.

Shen, C., Li, C.X., Li, X.M., Lu, Y.Z., Muhammad, Y., 2011. Chem. Eng. Sci. 66, 2690.

Shahriari, R., Dehghani, M.R., Behzadi, B., 2012. Ind. Eng. Chem. Res. 51, 10274.

Oliveira, M.B., Llovell, F., Coutinho, J.A.P., Vega, L.F., 2012. J. Phys. Chem. B. 116, 9089.

Hosseini, S.M., Moghadasi, J., Papari, M.M., Nobandegani, F.F., 2012. Ind. Eng. Chem. Res. 51, 758.

Yousefi, F., 2012. Ionics 18, 769.

Sheikhi-Kouhsar, M., Bagheri, H., Raeissi, S., 2015. Fluid Phase Equilibr. 395, 51.

Liu, H., Yang, F., Yang, Z., Duan, Y., 2020. J. Mol. Liq. 308, 113027.

Kamath, R.S., Biegler, L.T., Grossmann, I.E., 2010. Comput. Chem. Eng. 34, 2085.

Ghoderao, P.N.P., Dalvi, V.H., Narayan, M., 2019. Chem. Eng. Sci. 3, 100026.

Coquelet, C., Abbadi, J.E., Houriez, C., 2016. Int. J. Refrig. 69, 418.

Panayiotou, C., Zuburtikudis, I., Hatzimanikatis, V., 2019. Ind. Eng. Chem. Res. 58, 12787.

Farrokh-Niae, A.H., Moddarress, H., Mohsen-Nia, M., 2008. J. Chem. Thermodyn. 40, 84.

Kukreja, N., Ghoderao, P., Dalvi, V.H., Narayan, M., 2021. Fluid Phase Equilibr. 531, 112908.

Secuianu, C., Feroiu, V., Geană, D., 2008. J. Supercrit. Fluid 47, 109.

Lopez-Echeverry, J.S., Reif-Acherman, S., Araujo-Lopez, E., 2017. Fluid Phase Equilibr. 447, 39.

Perdomo, F.A., Khalit, S.H., Adjiman, C.S., Galindo, A., Jackson, G., 2021. AICHE J. 63, 17194.

Gross, J., Sadowski, G., 2002. Ind. Eng. Chem. Res. 41, 5510.

Bülow, M., Greive, M., Zaitsau, D.H., Verevkin, S.P., Held, C., 2021. Chemistry Open. 10, 216.

Qiao, Y., Ma, Y., Huo, Y., Ma, P., Xia, S., 2010. J. Chem. Thermodyn. 42, 852.

Peng, D., Zhang, J., Cheng, H., Chen, L., Qi, Z., 2017. Chem. Eng. Sci. 159, 58.

Chen, Y., Kontogeorgis, G.M., Woodley, S.M., 2019. Ind. Eng. Chem. Res. 58, 4277.

Venkatraman, V., Alsberg, B.K., 2017. J. CO$_2$ Util. 21, 162.

Zhang, S., Sun, N., He, X., Lu, X., Zhang, X., 2006. J. Phys. Chem. Ref. Data. 35, 1475.

Yusuf, F., Olayiwola, T., Afagwu, C., 2021. Fluid Phase Equilibr. 531, 112898.

Low, K., Kobayashi, R., Izgorodina, E.I., 2020. J. Chem. Phys. 153, 104101.

Valderrama, J.O., Sanga, W.W., Lazzús, J.A., 2008. Ind. Eng. Chem. Res. 47, 1318.

Danesh, A., 1998. PVT and phase behaviour of petroleum reservoir fluids. Elsevier.

Green, D.W., Southard, M.Z., 2019. Perry's chemical engineers' handbook. McGraw-Hill Education.

Mokhtarani, B., Sharifi, A., Mortaheb, H.R., Mirzaei, M., Mafi, M., Sadeghian, F., 2009. J. Chem. Thermodyn. 41, 323.

Wang, J.Y., Zhang, X.J., Hu, Y.Q., Liang, L.Y., 2012. J. Chem. Thermodyn. 45, 43.

Rilo, E., Pico, J., García-Garabal, S., Varela, L.M., Cabeza, O., 2009. Fluid Phase Equilibr. 285, 83.

Solanki, S., Hooda, N., Sharma, V.K., 2013. J. Chem. Thermodyn. 56, 123.

Bhagour, S., Solanki, S., Hooda, N., Sharma, D., Sharma, V.K., 2013. J. Chem. Thermodyn. 60, 76.

Bhattacharjee, A., Varanda, C., Freire, M.G., Matted, S., Santos, L.M., Marrucho, I.M., Coutinho, J.A., 2012. J. Chem. Eng. Data. 57, 3473.

Wang, J.Y., Zhao, F.Y., Liu, Y.M., Wang, X.L., Hu, Y.Q., 2011. Fluid Phase Equilibr. 305, 114.

Bhujrajh, P., Deenadayalu, N., 2007. J. Solution Chem. 36, 631.

Quijada-Maldonado, E., Van der Boogaart, S., Lijbers, J.H., Meindersma, G.W., De Haan, A.B., 2012. J. Chem. Thermodyn. 51, 51.

Rodriguez, H., Brennecke, J.F., 2006. J. Chem. Eng. Data. 51, 2145.

Wang, J.Y., Jiang, H.C., Liu, Y.M., Hu, Y.Q., 2011. J. Chem. Thermodyn. 43, 800.

Zhao, F.Y., Liang, L.Y., Wang, J.Y., Hu, Y.Q., 2012. Chin. Chem. Lett. 23, 1295.

Vercher, E., Orchilles, A.V., Miguel, P.J., Martínez-Andreu, A., 2007. J. Chem. Eng. Data. 52, 1468.

Sadeghi, R., Shekaari, H., Hosseini, R., 2009. Int. J. Thermophys. 30, 1491.

Tong, J., Liu, Q.S., Guan, W., Yang, J.Z., 2009. J. Chem. Eng. Data. 54, 1110.

Iglesias-Otero, M.A., Troncoso, J., Carballo, E., Romaní, L., 2008. J. Chem. Thermodyn. 40, 949.

Gao, H., Qi, F., Wang, H., 2009. J. Chem. Thermodyn. 41, 888.

Patel, H., Vaid, Z.S., More, U.U., Ijardar, S.P., Malek, N.I., 2016. J. Chem. Thermodyn. 99, 40.

Domańska, U., Pobudkowska, A., Wiśniewska, A., 2006. J. Solution Chem. 35, 311.

Kumar, B., Singh, T., Rao, K.S., Pal, A., Kumar, A., 2012. J. Chem. Thermodyn. 44, 121.

Mokhtarani, B., Mojtahedi, M.M., Mortaheb, H.R., Mafi, M., Yazdani, F., Sadeghian, F., 2008. J. Chem. Eng. Data. 53, 677.

Matkowska, D., Hofman, T., 2013. J. Mol. Liq. 177, 301.

Gao, H., Yu, Z., Wang, H., 2010. J. Chem. Thermodyn. 42, 640.

Jiang, H., Zhao, Y., Wang, J., Zhao, F., Liu, R., Hu, Y., 2013. J. Chem. Thermodyn. 64, 1.

Singh, S., Aznar, M., Deenadayalu, N., 2013. J. Chem. Thermodyn. 57, 238.

Pau, S., Panda, A.K., 2012. Colloids Surf. A Physicochem. Eng. Asp. 404, 1.

Wandschneider, A., Lehmann, J.K., Heintz, A., 2008. J. Chem. Eng. Data. 53, 596.

Zhong, Y., Wang, H., Diao, K., 2007. J. Chem. Thermodyn. 39, 291.

Fan, W., Zhou, Q., Sun, J., Zhang, S., 2009. J. Chem. Eng. Data. 54, 2307.

Pal, A., Kumar, B., 2011. J. Mol. Liq. 163, 128.

Pal, A., Gaba, R., Singh, T., Kumar, A., 2010. J. Mol. Liq. 154, 41.

Kermanpour, F., Sharifi, T., 2012. Thermochim. Acta. 527, 211.

Kermanpour, F., 2012. J. Mol. Liq. 169, 156.

Kermanpour, F., Niakan, H.Z., 2012. J. Chem. Thermodyn. 48, 129.

Pal, A., Kumar, B., 2012. Fluid Phase Equilibr. 334, 157.

Zhu, A., Wang, J., Liu, R., 2011. J. Chem. Thermodyn. 43, 796.

Gomez, E., Gonzalez, B., Domínguez, Á., Tojo, E., Tojo, J., 2006. J. Chem. Eng. Data. 51, 696.

Malek, N.I., Singh, A., Surati, R., Ijardar, S.P., 2014. J. Chem. Thermodyn. 74, 103.

Ijardar, S.P., Malek, N.I., 2014. J. Chem. Thermodyn. 71, 236.

Akbar, M.M., Murugesan, T., 2013. J. Mol. Liq. 177, 54.

Akbar, M.M., Chemat, F., Arunagiri, A., Murugesan, T., 2016. J. Therm. Anal. Calorim. 123, 785.

González, E.J., Domínguez, Á., Macedo, E.A., 2012. J. Chem. Thermodyn. 47, 300.

Pereiro, A.B., Tojo, E., Rodrıguez, A., Canosa, J., Tojo, J., 2006. J. Chem. Thermodyn. 38, 651.

Pereiro, A.B., Rodriguez, A., 2007. J. Chem. Thermodyn. 39, 978.

Jiang, H., Wang, J., Zhao, F., Qi, G., Hu, Y., 2012. J. Chem. Thermodyn. 47, 203.

Bagheri, H., Mansoori, G.A., Hashemipour, H., 2018. J. Mol. Liq. 261, 174.

Soave, G., 1984. Chem. Eng. Sci. 39, 357.

Redlich, O., Kwong, J.N., 1949. Chem. Rev. 44, 233.

Soave, G., 1972. Chem. Eng. Sci. 27, 1197.

Soave, G., Barolo, M., Bertucco, A., 1993. Fluid Phase Equilibr. 91, 87.

Peng, D.Y., Robinson, D.B., 1976. Ind. Eng. Chem. Fundam. 15, 59.

Gaffney, J.A., Hu, S.X., Arnault, P., Becker, A., Benedict, L.X., Boehly, T.R., Celliers, P.M., Ceperley, D.M., Čertík, O., Clérouin, J., Collins, G.W., 2018. High Energ. Dens. Phys. 28, 7.

Bagheri, H., Hashemipour, H., Mirzaie, M., 2019. J. Mol. Liq. 281, 490.

Yang, F., Liu, Q., Duan, Y., Yang, Z., 2018. Chem. Eng. Sci. 192, 565.

Yokozeki, A., Shiflett, M.B., 2010. J. Supercrit. Fluid 55, 846.

Bagheri, H., Hashemipour, H., Ghader, S., 2019. Comput. Part. Mech. 6, 721.

Kumar, A., Upadhyay, R., 2021. Chem. Eng. Sci. 229, 116045.

Schmidt, G., Wenzel, H., 1980. Chem. Eng. Sci. 35, 1503.

Patel, N.C., Teja, A.S., 1982. Chem. Eng. Sci. 37, 463.

Ghalandari, V., Hashemipour, H., Bagheri, H., 2020. Fluid Phase Equilib. 508, 112433.

El shafiee, C.E., El-Nagar, R.A., Nessim, M.I., Khalil, M.M.H., Shaban, M.E., Alharthy, R.D., Ismail, D.A., Abdallah, R.I., Moustafa, Y.M., 2021. Arab. J. Chem. 14, 103123.

Elbro, H.S., Fredenslund, A., Rasmussen, P., 1991. Ind. Eng. Chem. Res. 30, 2576.

Mchaweh, A., Alsaygh, A., Nasrifar, K., Moshfeghian, M., 2004. Fluid Phase Equilibr. 224, 157.

Gunn, R.D., Yamada, T., 1971. AIChE J. 17, 1341.

Hankinson, R.W., Thomson, G.H., 1979. AIChE J. 25, 653.

B. E. Poling, J. M. Prausnitz, J. P. O'connell, The properties of liquids and gases. New York. 2001.

Sandler, S.I., 2017. Chemical, biochemical, and engineering thermodynamics. John Wiley & Sons.

Kontogeorgis, G.M., Folas, G.K., 2009 Dec 1. Thermodynamic models for industrial applications: from classical and advanced mixing rules to association theories. John Wiley & Sons.

Nasrifar, K., Moshfeghian, M., 1998. Fluid Phase Equilibr. 153, 231.

Rabari, D., Patel, N., Joshipura, M., Banerjee, T., 2014. Chem. Eng. Data. 59, 571.

Mathias, P.M., Copeman, T.W., 1983. Fluid Phase Equilibr. 13, 91.

Memarzadeh, R., Zadeh, H.G., Dehghani, M., Riahi-Madvar, H., Seifi, A., Mortazavi, S.M., 2020. Sci. Total Environ. 716, 137007.

Ali, M., Deo, R.C., Downs, N.J., Maraseni, T., 2018. Atmos. Res. 213, 450.

Nguyen-Huy, T., Deo, R.C., Mushtaq, S., An-Vo, D.A., Khan, S., 2018. Eur. J. Agron. 98, 65.

Xu, X., Liang, T., Zhu, J., Zheng, D., Sun, T., 2019. Neurocomputing. 328, 5.

Riahi-Madvar, H., Seifi, A., 2018. Arab. J. Geosci. 11, 1.

Loey, M., Manogaran, G., Taha, M.H.N., Khalifa, N.E.M., 2021. Measurement. 167, 108288.

Mueller, J.P., Massaron, L., 2021. Machine learning for dummies. John Wiley & Sons.

Lajiness, M., Watson, I., 2008. Curr. Opin. Chem. Biol. 12, 366.

Kennard, R.W., Stone, L.A., 1969. Technometrics 11, 137.

Riahi-Madvar, H., Dehghani, M., Seifi, A., Singh, V.P., 2019. Water Resour. Manag. 33, 905.

Wu, W., Walczak, B., Massart, D.L., Heuerding, S., Erni, F., Last, I. R., Prebble, K.A., 1996. Chemometr. Intell. Lab. 33, 35.

Singh, A., 2019. Eng. Manag. J. 10, 713.

Mirjalili, S., Lewis, A., 2016. Adv. Eng. Softw. 95, 51.

Liakos, K.G., Busato, P., Moshou, D., Pearson, S., Bochtis, D., 2018. Sensors. 18, 2674.

Kotsiantis, S.B., Zaharakis, I.D., Pintelas, P.E., 2006. Artif. Intell. Rev. 26, 159.

Dutton, D.M., Conroy, G.V., 1997. Knowl. Eng. Rev. 12, 341.

Maxwell, A.E., Warner, T.A., Fang, F., 2018. Int. J. Remote Sens. 39, 2784.